MICROBIOLOGY

The fibrinolytic system enables the onset of *Plasmodium* infection in the mosquito vector and the mammalian host

Thiago Luiz Alves e Silva[1,2]*, Andrea Radtke[3], Amanda Balaban[1†], Tales Vicari Pascini[4], Zarna Rajeshkumar Pala[4], Alison Roth[5], Patricia H. Alvarenga[1,2‡], Yeong Je Jeong[4], Janet Olivas[4], Anil K. Ghosh[1§], Hanhvy Bui[1‖], Brandon S. Pybus[5], Photini Sinnis[1], Marcelo Jacobs-Lorena[1¶#], Joel Vega-Rodríguez[1*¶#]

Plasmodium **parasites must migrate across proteinaceous matrices to infect the mosquito and vertebrate hosts. Plasmin, a mammalian serine protease, degrades extracellular matrix proteins allowing cell migration through tissues. We report that *Plasmodium* gametes recruit human plasminogen to their surface where it is processed into plasmin by corecruited plasminogen activators. Inhibition of plasminogen activation arrests parasite development early during sexual reproduction, before ookinete formation. We show that increased fibrinogen and fibrin in the blood bolus, which are natural substrates of plasmin, inversely correlate with parasite infectivity of the mosquito. Furthermore, we show that sporozoites, the parasite form transmitted by the mosquito to humans, also bind plasminogen and plasminogen activators on their surface, where plasminogen is activated into plasmin. Surface-bound plasmin promotes sporozoite transmission by facilitating parasite migration across the extracellular matrices of the dermis and of the liver. The fibrinolytic system is a potential target to hamper *Plasmodium* transmission.**

INTRODUCTION

Plasmodium parasites are the etiological agents of malaria and are transmitted to humans by the bite of infected *Anopheles* mosquitoes. After ingestion of an infected blood meal, *Plasmodium* male and female gametes mate in the mosquito midgut giving rise to zygotes, which, in turn, differentiate into motile ookinetes (fig. S1A). Ookinetes transverse the mosquito midgut epithelium and differentiate into oocysts (*1*, *2*). Each oocyst undergoes sporogony to form thousands of sporozoites that are released into the hemolymph, from where they specifically invade the salivary glands (fig. S1A). During probing and blood feeding, an infected mosquito deposits sporozoites into the dermis (fig. S1B). Infection requires sporozoites to migrate through the dermis, to find and enter a blood vessel to be carried to the liver, where they exit the circulation to invade hepatocytes and initiate a blood stage infection (fig. S1B) (*3*). Throughout the *Plasmodium* life cycle, the parasite encounters multiple physical barriers. In the mosquito, these include a compacted blood bolus, the chitin-rich peritrophic matrix, the midgut microvilli-associated network and mucins (*4*–*6*), and the midgut epithelium. In the mammalian host, barriers include the extracellular matrix of the dermis, the basement lamina of blood vessels, the endothelial and Kupffer cells of the liver blood vessels, the extracellular matrix of the liver space of Disse, and the hepatocyte membranes (fig. S1, A and B) (*7*). Whereas the motile stages of the malaria parasite rely on an actomyosin-based motor (the glideosome) to generate the forces required for migration (*8*), these forces are unlikely to be sufficient to break through the intricate extracellular matrices.

The human fibrinolytic system consists of two main protein classes: serine proteases that ultimately degrade fibrin (fibrinogen-derived polymers) and dissolve clots and serpins that tightly regulate the activity of these proteases (*9*). Plasminogen is the precursor of plasmin, a potent serine protease that cleaves a broad spectrum of substrates and is the effector protease of the fibrinolytic system. Plasmin can bind to lysine motifs of proteins exposed on the cell surface (*9*). Surface-associated plasmin broadly facilitates cell migration via digestion of connective tissue and extracellular matrix proteins, as is the case for leukocyte infiltration of inflammatory sites (*10*), tumor growth and metastasis (*11*), embryogenesis (*12*), and pathogen invasion of host tissues (*13*). Plasminogen is proteolytically activated into plasmin by plasminogen activators, namely, tissue-type plasminogen activator (tPA) and urokinase-type plasminogen activator (uPA) (*9*). These two proenzymes constitutively circulate in the blood and have low intrinsic catalytic activity (*9*). The activation of cell-associated plasminogen occurs when plasminogen and its activators bind to receptors on the cell surface, bringing the activators and plasminogen into close proximity (*14*). In a positive feedback loop, plasmin further activates both tPA and uPA, thus accelerating and amplifying plasminogen activation. The serpin plasminogen activator inhibitor-1 (PAI-1) regulates plasminogen activation by

[1]The W. Harry Feinstone Department of Molecular Microbiology and Immunology and Johns Hopkins Malaria Research Institute, Bloomberg School of Public Health, Johns Hopkins University, Baltimore, MD 21205, USA. [2]Laboratório de Bioquímica de Resposta ao Estresse, Instituto de Bioquímica Médica, Universidade Federal do Rio de Janeiro, Rio de Janeiro 21941-902, Brazil. [3]Laboratory of Immune System Biology, National Institute of Allergy and Infectious Diseases, National Institutes of Health, Bethesda, MD 20814, USA. [4]Laboratory of Malaria and Vector Research, National Institute of Allergy and Infectious Diseases, National Institutes of Health, Rockville, MD 20852, USA. [5]Department of Drug Discovery, Experimental Therapeutics Branch, Walter Reed Army Institute of Research, Silver Spring, MD 20910, USA.
*Present address: Laboratory of Malaria and Vector Research, National Institute of Allergy and Infectious Diseases, National Institutes of Health, Rockville, MD 20852, USA.
†Present address: Department of Cell Biology, Johns Hopkins School of Medicine, Johns Hopkins University, Baltimore, MD 21205, USA.
‡Present address: Structural Biology Section, Research Technologies Branch, National Institute of Allergy and Infectious Diseases, National Institutes of Health, Rockville, MD, USA.
§Deceased.
‖Present address: Integrated Imaging Center, Johns Hopkins University, Baltimore, MD 21218, USA.
¶These authors contributed equally to this work.
#Corresponding author. Email: ljacob13@jhu.edu (M.J.-L.); joel.vega-rodriguez@nih.gov (J.V.-R.)

specifically inhibiting the activity of both plasminogen activators but not of plasmin (*15*). PAI-1 constitutively circulates in the blood at low levels, and its expression is strongly up-regulated during inflammation, which contributes to the tight control of plasminogen activation (*16*, *17*).

In a previous report, Ghosh *et al.* (*18*) proposed that the recruitment of plasminogen to the surface of *Plasmodium berghei* and *Plasmodium falciparum* ookinetes is important for oocyst formation. Notably, the depletion of plasminogen from human blood severely reduced oocyst formation, implying that plasmin is essential for mosquito midgut invasion. Likewise, several pathogenic microorganisms including bacteria, fungi, and pathogenic protozoans have evolved mechanisms to co-opt plasminogen from their hosts and use its enzymatic activity to facilitate evasion of immune responses and invasion and dissemination through host tissue (*13*, *19*). Despite the major role played by plasminogen in *Plasmodium* infection of the mosquito, the mechanism of plasminogen activation, the molecular targets of parasite-associated plasmin, and the role of the fibrinolytic system at other *Plasmodium* developmental stages are currently unknown.

Here, we show that the malaria parasite recruits the host fibrinolytic system to facilitate infection of both the vector and the mammalian host. In the mosquito, plasmin enables parasite sexual reproduction, while in the mammalian host, sporozoites use plasmin to exit the skin and enter the liver. Targeting parasite plasmin utilization is a potential strategy to prevent malaria transmission.

RESULTS

Inhibition of plasminogen activators negatively affects ookinete formation

Oocyst formation is strongly reduced when gametocytes are fed to mosquitoes in plasminogen-depleted blood (*18*). Recombinant plasminogen added to depleted blood rescues oocyst development, whereas recombinant plasminogen carrying a point mutation (S741A) in the plasmin catalytic triad does not (*18*). However, no information was available for how plasminogen is activated into plasmin. We hypothesized that *P. falciparum* uses the human plasminogen activators to convert its cell-associated plasminogen into plasmin. To test this hypothesis, *P. falciparum* gametocytes were fed to mosquitoes with PAI-1, a serpin that specifically inhibits both tPA and uPA but not plasmin. PAI-1 inhibited midgut oocyst formation (Fig. 1A). The inhibition was reversed by the addition of plasmin to the infectious blood meal containing PAI, indicating that PAI itself does not directly interfere with *Plasmodium* development in the mosquito. Supplementation of the infectious blood meal with plasmin does not change parasite infection (fig. S2, D and E), indicating that the amount of plasmin(ogen) is not limiting. Addition of PAI-1 and/or plasmin to the blood meal does not affect the amount of blood ingested by the mosquito (fig. S3).

Previous and current findings show that plasmin activity is required for *P. falciparum* to form oocysts (*18*); however, it was unknown which parasite developmental stage preceding oocyst formation is affected by the absence of plasmin. To determine whether plasmin is required for gametogenesis, we induced gametocyte activation in vitro in the presence or absence of PAI-1. Detection of Pfs25-positive round cells was used as readout for female gamete activation, as *P. falciparum* changes from a Pfs25-negative falciform gametocyte to a round Pfs25-positive female gamete after activation (fig. S1A) (*20*). PAI-1 treatment did not change the number of round forms (female gametes or zygotes), indicating that the activation of female gametocytes into gametes was unaffected (Fig. 1B). To test whether PAI-1 affects ookinete formation, we fed mosquitoes with infected blood supplemented with PAI-1 and counted the number ookinetes (Pfs25-positive banana-shaped cells) in the blood bolus at around 23 hours after feeding (fig. S1A). PAI-1 treatment strongly reduced ookinete formation (Fig. 1B). To exclude PAI toxicity to the parasite, we investigated the effect of PAI on ookinete formation in vitro, using the *P. berghei* model. PAI was added to ookinete cultures before gamete activation. Ookinete formation in vitro was not affected by PAI-1 (Fig. S4, A and B), confirming that PAI-1 is not toxic to the parasite and that the inhibitory effect of PAI-1 only occurs in the mosquito blood bolus, under high viscosity conditions (considered further below). The PAI-1 serpin inhibitory activity of tPA was verified and confirmed (fig. S4C). These results suggest that the human plasminogen activators are essential for activating plasminogen into plasmin, which, in turn, is important for early stages of parasite development in the mosquito, likely fertilization.

To directly investigate the role of plasminogen activators during mosquito infection, we used different strategies to modulate either their concentration or activity in the infective blood. First, mosquitoes were infected using tPA-depleted blood. The absence of tPA strongly reduced oocyst numbers (Fig. 1C), and this decrease was reversed in a dose-dependent manner by supplementing the infectious tPA-depleted blood with increasing concentrations of recombinant single-chain tPA (sc-tPA; the tPA proenzyme) (Fig. 1C). Moreover, supplementation of normal blood with the tPA inhibitor, PPACK (*21*), also reduced oocyst numbers in a dose-dependent manner (fig. S2A). To further explore the role of tPA during midgut infections, we supplemented infectious blood with active tPA [two-chain tPA (tc-tPA)] that significantly increased oocyst numbers in a dose-dependent manner (Fig. 1D), suggesting that tPA availability limits parasite development in the mosquito gut. Together, these results suggest that tPA is important for *P. falciparum* infection of the mosquito midgut.

To test the importance of uPA for midgut infection, infectious blood was supplemented with the uPA inhibitor, DGGACK (*22*), and the effect on oocyst formation was determined. Oocyst numbers decreased in a dose-dependent manner (Fig. 1E). In addition, supplementation of infective blood with an anti-uPA antibody significantly inhibited midgut infection (fig. S2B) (*23*). Next, we tested whether supplementation with active uPA (two-chain uPA, tc-uPA) would positively affect midgut infection. The addition of tc-uPA to infective blood did not significantly affect oocyst numbers (Fig. 1F), suggesting that uPA availability is not limiting for parasite development in the mosquito gut. Likewise, the addition of tranexamic acid, a lysine analog that inhibits the binding of tPA and plasminogen to protein lysine residues, decreased the infection in a dose-dependent manner (fig. S2C). Collectively, these results show that the human plasminogen activators play a critical role during *P. falciparum* development in the midgut.

Plasminogen activators bind to the surface of *P. falciparum* sexual-stage parasites

Activation of cell-associated plasminogen depends on the recruitment of plasminogen activators to the cell surface, thus placing them in close proximity to plasminogen (*24*). Using immunofluorescence assays (IFAs), we found that both plasminogen and tPA bind to and

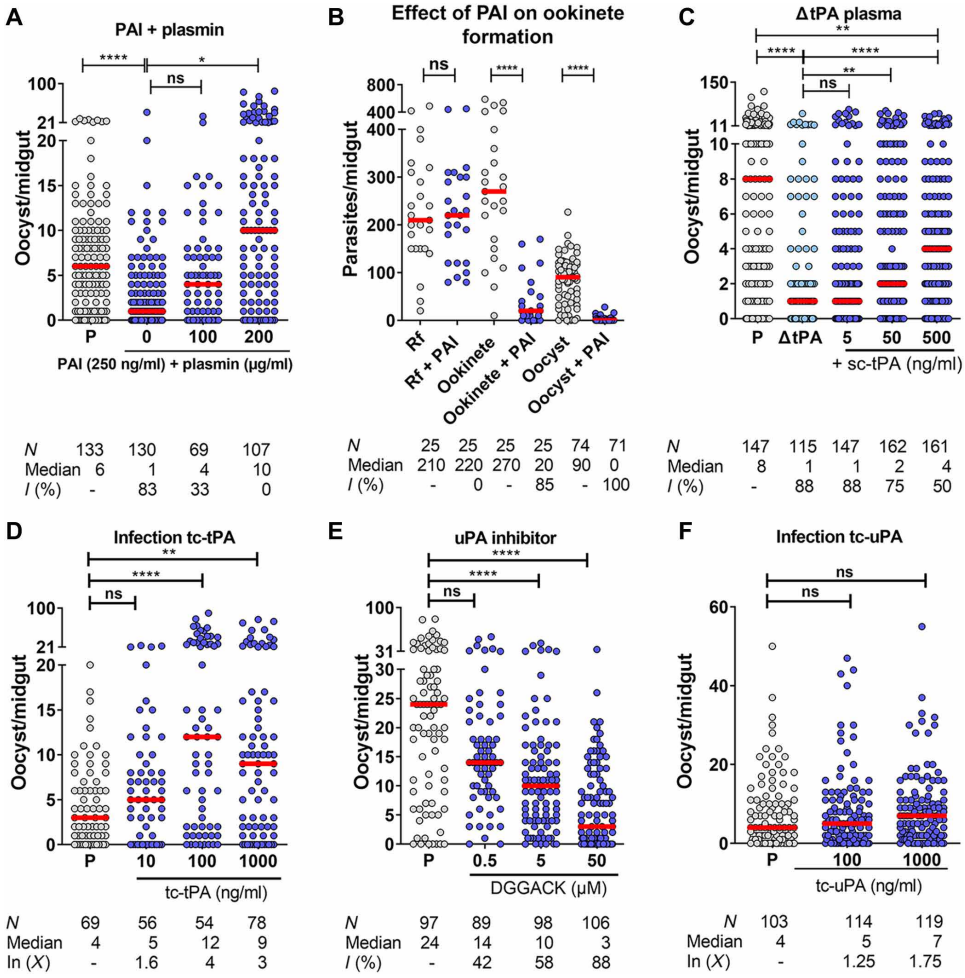

Fig. 1. Plasminogen activators are required for *P. falciparum* mosquito infection. *An. gambiae* mosquitoes were fed on infected blood reconstituted with human plasma and supplemented with the indicated inhibitors, agonists, or phosphate-buffered saline (PBS). Mosquito midguts were dissected 10 days later, and oocysts were counted. (**A**) PAI-1 inhibits oocyst formation in *An. gambiae* mosquitoes. Plasmin supplementation reverses the PAI-1 inhibition. Data pooled from three independent experiments. (**B**) PAI-1 (2.5 µg/ml) does not inhibit gametogenesis (round form formation) but inhibits ookinete formation. Round forms (Rf; female gametes plus zygotes) and ookinetes were isolated from the midgut blood bolus and counted at 22 to 23 hours and oocysts at 10 days after infection. Data are pooled from three independent experiments. (**C**) tPA-depleted plasma (ΔtPA) negatively affects oocyst development and supplementation with single-chain tPA (sc-tPA; the pro-enzyme) partially rescues the inhibition. Data pooled from four independent experiments. (**D**) Addition of active tc-tPA to an infectious blood meal increases oocyst development. Data pooled from three independent experiments. (**E**) The uPA inhibitor DGGACK reduces oocyst development. Data are pooled from two independent experiments. (**F**) Addition of active two-chain uPA (tc-uPA) to an infectious blood meal does not increase oocyst development. Data pooled from four independent experiments. *N*, number of midguts; *I* (%), percent inhibition; ln (*X*), fold increase; ΔtPA, tPA-depleted plasma; P, plasma; red horizontal lines, medians. Kruskal-Wallis with Dunn's posttest. $^{*}P < 0.05$, $^{**}P < 0.01$, $^{****}P < 0.0001$; ns, not significant.

colocalize on the surface of male gametes, female gametes, zygotes, and ookinetes (Fig. 2A and fig. S5A). Likewise, uPA binds to male gametes and zygotes, where it also colocalizes with plasminogen (Fig. 2B and fig. S5A).

Plasminogen and tPA contain kringle domains that mediate the binding to exposed lysine residues on cell surface receptors (*25*). To test the specificity of plasminogen and tPA binding to *Plasmodium* parasites, female gametes were incubated with plasminogen or tPA in the presence of the lysine analog tranexamic acid, and binding of the activators to the parasite was analyzed by IFA. Tranexamic acid strongly inhibited the binding of plasminogen and tPA to female gametes (Fig. 2C). These results suggest that the interaction of tPA and plasminogen with the parasite is mediated by their kringle domains.

To test whether tPA is required for activation of parasite-associated plasminogen, we measured plasmin activity on the surface of female gametes. Mature gametocytes were activated in vitro in RPMI 1640 supplemented with 10% Albumax and 100 µM xanthurenic acid, and the resulting female gametes were purified 1 hour after activation (fig. S5B). Albumax is a lipid-rich bovine serum albumin (BSA) that does not contain plasminogen or plasminogen activators. Female gametes activated in the presence of Albumax were negative for tPA and plasminogen as evaluated by Western blot (Fig. S5, C and D). To measure plasmin activity, female gametes were incubated in the presence of recombinant sc-tPA for 1 hour, washed to remove unbound sc-tPA, and then incubated with plasminogen. After 1 hour, unbound plasminogen was removed by washing, and then plasmin

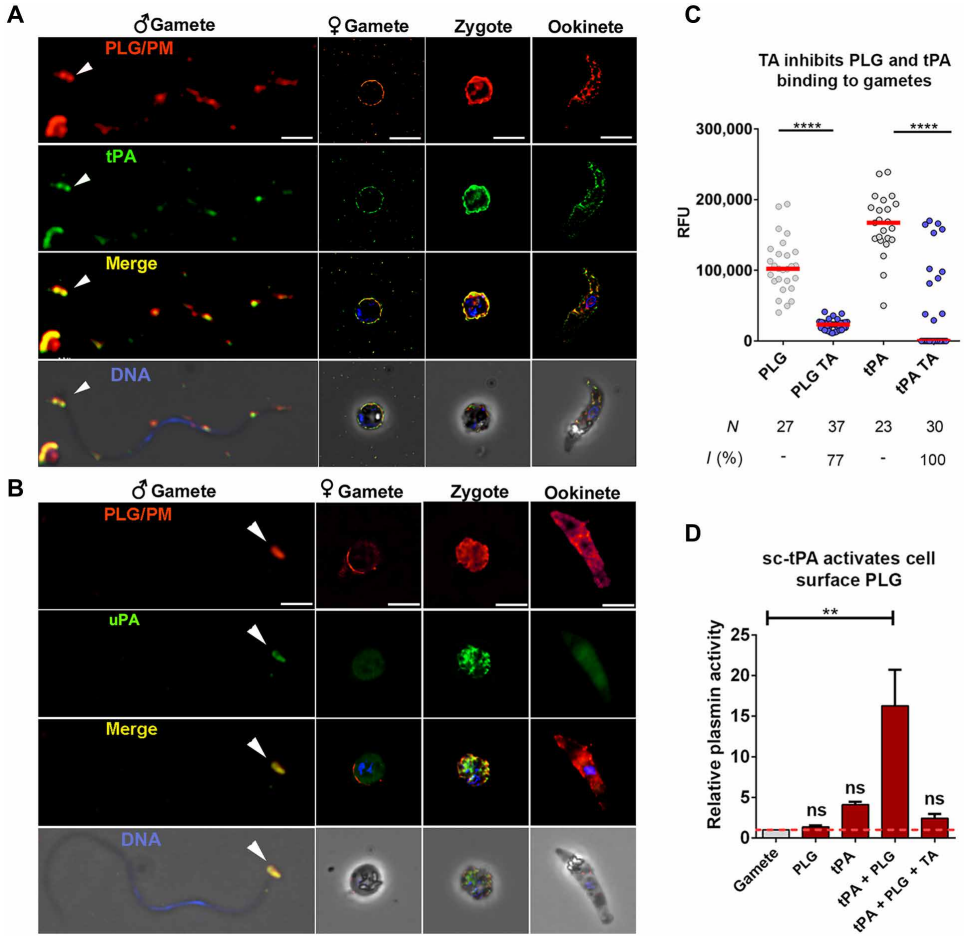

Fig. 2. Plasminogen, tPA, and uPA bind to the surface of *P. falciparum* sexual stages. (**A** and **B**) Plasminogen (PLG), tPA (A), and uPA (B) bind to male (♂) and female (♀) gametes, zygotes, and ookinetes. Immunofluorescence images merged with phase contrast images in the bottom row. White arrowheads point to localization of plasminogen and plasminogen activators on the heads of microgametes. Scale bars for male gametes, 2 μm; scale bars for female gametes, zygotes and ookinetes, 6 μm. (**C**) The lysine analog tranexamic acid (TA) inhibits tPA and PLG association with the parasite surface. Purified female gametes were incubated with PLG and tPA in the presence or absence of TA. Plasminogen and tPA binding were determined by IFA with an anti-PLG and an anti-tPA antibody. Data pooled from two independent experiments. *N*, number of midguts; *I* (%), percent inhibition; RFU, relative fluorescence units. (Mann-Whitney *U* test, ****$P < 0.0001$). (**D**) tPA activates plasminogen on the surface of female gametes. Female gametes were incubated with the sc-tPA proenzyme. After binding, the cells were washed and incubated with PLG. Plasmin activity was measured using a chromogenic substrate. Controls: Gametes were incubated with either PBS, PLG, sc-tPA alone, or with sc-tPA followed by PLG in the presence of TA. Error bars represent SEM from three independent experiments. Analysis of variance (ANOVA) followed by Tukey's multiple comparison test. **$P < 0.01$.

activity was measured using a colorimetric substrate (*26*). Strong plasmin activity was detected in parasites incubated with sc-tPA and plasminogen, but not in parasites incubated with either sc-tPA or plasminogen alone (Fig. 2D). Incubation of parasites with sc-tPA plus tranexamic acid, before incubation with plasminogen, abolished surface plasmin activity, supporting our previous results indicating that tPA binds to the parasite surface via its kringle domain. These results suggest that tPA is sufficient for plasminogen activation on the parasite surface.

Fibrinogen and fibrin polymerization increase the blood bolus viscosity

During blood feeding, *Anopheles* mosquitoes perform diuresis (excretion of excess fluid via the urine), which allows the mosquito to ingest a large volume of blood (*27*). As a result, the concentration of blood cells and proteins increase in the midgut bolus (*28*). Fibrinogen, one of the most abundant blood proteins, interacts with activated platelets (*29*), red blood cells (RBCs) (*30*), and leukocytes (*31*), mediating spontaneous aggregation (fig. S6A). Serum contains lower concentrations of fibrinogen and clotting factors compared to plasma, as serum is prepared from coagulation of plasma (*32*). Western blot analysis of midgut blood boluses shows a higher amount of fibrinogen in mosquitoes fed with RBCs reconstituted with plasma than with serum (fig. S6B). In addition, the viscosity of the RBC suspension reconstituted with plasma or Albumax plus fibrinogen was higher than RBCs reconstituted with serum or with Albumax alone, respectively (fig. S6, C and D).

To evaluate whether fibrinogen is converted to fibrin during blood feeding, the midgut contents from mosquitoes fed on RBCs reconstituted in different media (plasma, serum, Albumax, or Albumax supplemented with fibrinogen) were analyzed by Western blotting 15 min and 1 hour after feeding, using an antibody that detects fibrin polymers. Typical markers of fibrin, namely, γ-γ dimers (94 to 97 kDa) and α-polymers (120 kDa up to 770 kDa) (*33*, *34*), were

detected in the blood bolus at 15 min and 1 hour after blood feeding with plasma. The polymers were detected at much lower intensity in serum and were absent in Albumax or Albumax plus fibrinogen (Fig. 3, A and B). Reduced levels of fibrin polymers are expected in serum due to the removal of the fibrin clot during serum preparation and in Albumax due to the absence of coagulation factors. The same markers were detected at 1 hour after blood feeding but at lower intensity. Fibrin formation in the midgut bolus was more pronounced when mosquitoes were fed directly on a mouse—in the absence of anticoagulants—implying that clotting factors are active in the blood bolus (Fig. 3, A and B). These results show that fibrin is formed in the mosquito blood bolus, despite the presence of anticoagulants from the mosquito saliva that is ingested during blood feeding (*35*, *36*).

Next, we tested whether the higher concentration of fibrinogen in plasma and the subsequent polymerization of fibrin in the mosquito midgut correlate with higher RBC aggregation in the blood bolus. Midguts from mosquitoes fed with RBCs reconstituted with either serum or plasma were disrupted in phosphate-buffered saline (PBS) 15 min after feeding, and RBC rouleaux structures (rosettes) were analyzed by ImageStream flow cytometry. Blood obtained from mosquitoes that fed on RBCs in plasma had a significantly higher proportion of RBC aggregates (small clumps and rosettes) than midguts from mosquitoes fed on RBCs in serum (Fig. 3, C and D, and fig. S6E). These observations suggest that the fibrinogen present in the plasma induces RBC aggregation in the blood bolus, in consonance with the in vitro results (fig. S6A). To test whether the effect of clumping was due to the presence of fibrinogen, mosquito midguts fed with RBCs reconstituted with either Albumax or Albumax supplemented with fibrinogen were analyzed by ImageStream flow cytometry. Albumax plus fibrinogen induced higher RBC clumping than Albumax alone (Fig. 3E). Together, our results suggest that limited fibrin polymerization and fibrinogen-mediated RBC clumping occur in the mosquito gut within minutes after blood feeding, which could impose a barrier to parasite motility.

Fibrinogen is associated with decreased *P. falciparum* infectivity

We hypothesized that the high viscosity of the blood bolus caused by the increased fibrinogen concentration and fibrin polymerization after diuresis will negatively affect *Plasmodium* development in

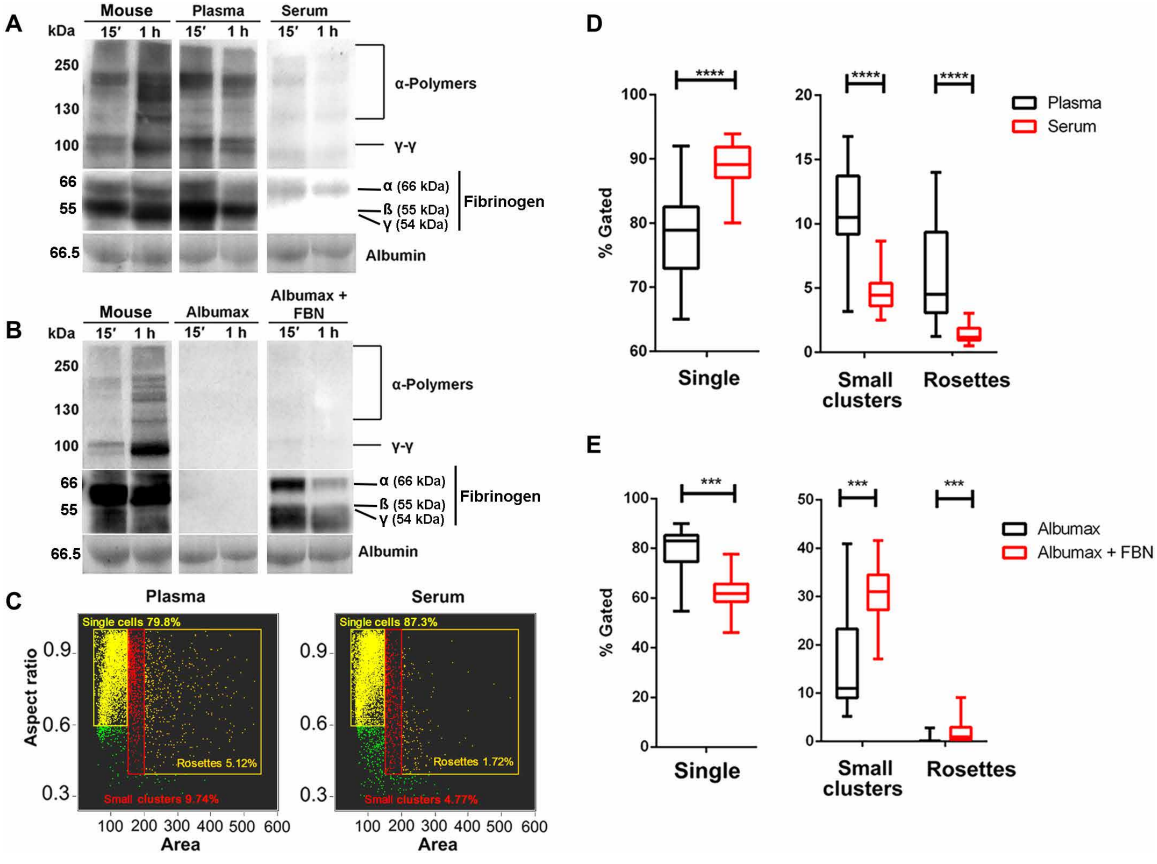

Fig. 3. Detection of fibrin and RBC aggregates in mosquito midguts. (**A** and **B**) Western blot showing the detection of fibrin in the blood bolus of mosquitoes fed directly on a mouse or human RBCs reconstituted with (A) plasma or serum or (B) Albumax or Albumax plus fibrinogen (FBN; 4 mg/ml). Anti-human fibrinogen antibody detects fibrin—γ-γ dimers (95 kDa) and α-polymers (>120 kDa). Albumin from the Ponceau stained membrane was used as loading control. (**C**) Representative ImageStream flow cytometry plots of RBC aggregation in one mosquito midgut blood bolus (related to fig. S6C) 15 min after feeding on human RBCs supplemented with either plasma or serum. (**D**) The percentage of intermediate clumps and RBC rosettes in the midgut blood bolus is higher with plasma as compared to serum [related to (C)] (18 midguts analyzed for both conditions). (**E**) Same experimental setup as in (D) showing an increase of small clusters and RBC rosettes in the blood bolus of mosquitoes fed on human RBCs suspended in Albumax plus fibrinogen (13 midguts analyzed) when compared to Albumax alone (12 midguts analyzed). Mann-Whitney test, ***$P < 0.001$, ****$P < 0.0001$. Plasma was collected in sodium citrate.

the midgut. To address this question, we compared oocyst numbers in mosquitoes fed on infective blood reconstituted with either plasma or serum. Plasma and serum obtained from three different donors and adjusted to the same final concentration of sodium citrate (anticoagulant) were used to feed *P. falciparum* gametocytes to mosquitoes. In each case, we found that mosquitoes fed on serum had higher oocyst numbers than mosquitoes fed on plasma from the same individual (Fig. 4A). Next, we compared the effect of different concentrations of plasma fibrinogen on parasite infectivity. Oocyst loads were determined in mosquitoes fed with the same infective blood reconstituted with commercial plasma supplemented with increasing concentrations of fibrinogen (2 and 4 mg/ml). Higher fibrinogen concentrations significantly decreased oocyst numbers in mosquitoes infected with low (Fig. 4B) or high parasite numbers (Fig. 4C). We also assessed the effect of inhibiting the plasminogen activators on oocyst formation by adding PAI-1 to plasma and serum. While PAI-1 strongly reduced oocyst load in infections done with plasma (63% reduction, $P < 0.001$), the reduction in infections with serum was less pronounced (32%, $P < 0.0139$) (Fig. 4D). The reduction in infection induced by PAI-1 in serum can be explained by residual fibrinogen that is not completely removed by clotting during serum isolation. After ingesting RBCs in serum, mosquito diuresis increases the concentration of the residual fibrinogen that polymerizes into fibrin in the absence of anticoagulants (Fig. 3A), thereby interfering with parasite development. This is in agreement with previous results showing that PAI-1 does not affect ookinete formation in vitro (fig. S4). In culture, PAI-1 should not affect fertilization since the high viscosity of the blood bolus does not exist due to the addition of anticoagulants and the dilution of fibrinogen by the culture medium, providing a fluid environment where gamete motility is not curtailed. Since fibrinogen and fibrin are natural substrates for plasmin, we propose as a working model that *Plasmodium* parasites use their surface-associated plasmin activity to cleave fibrinogen and fibrin in the blood bolus to facilitate parasite movement within the blood bolus.

Plasminogen activation is required for sporozoite infectivity of the mammalian host

For successful infection of the mammalian host, the sporozoite must overcome physical barriers imposed by extracellular matrices of the skin and liver. We first investigated whether the fibrinolytic enzymes bind to the sporozoite and, if so, whether plasminogen can be activated at its surface. We found that plasminogen, tPA, and uPA all bind to *P. falciparum* and *P. berghei* sporozoites when incubated with plasma (Fig. 5, A and B, and fig. S7). In addition, plasmin activity can be detected at the sporozoite surface after incubation with plasminogen and tPA but not with plasminogen alone (Fig. 5C). This activity was blocked by preincubation of tPA with tranexamic acid (Fig. 5C), suggesting that tPA interaction with the sporozoite is specific and is mediated by its kringle domain. To determine whether plasminogen activation is required for sporozoite infectivity, mice were injected intravenously with PAI-1 and challenged 1 hour later with the bite of three *P. berghei*–infected mosquitoes. PAI-1 treatment results in a 52% reduction of the number of mice that develop blood stage infection (Fig. 5D). The infection rate was restored by coinjection of plasmin and PAI-1 (Fig. 5D). These data indicate that plasminogen activation plays a crucial role for infection of the mammalian host.

Plasminogen activation facilitates motility of sporozoites delivered to the skin

Reduced sporozoite infection by mosquito bite (Fig. 5D) could result from inhibition of sporozoite exit from the skin or inhibition of

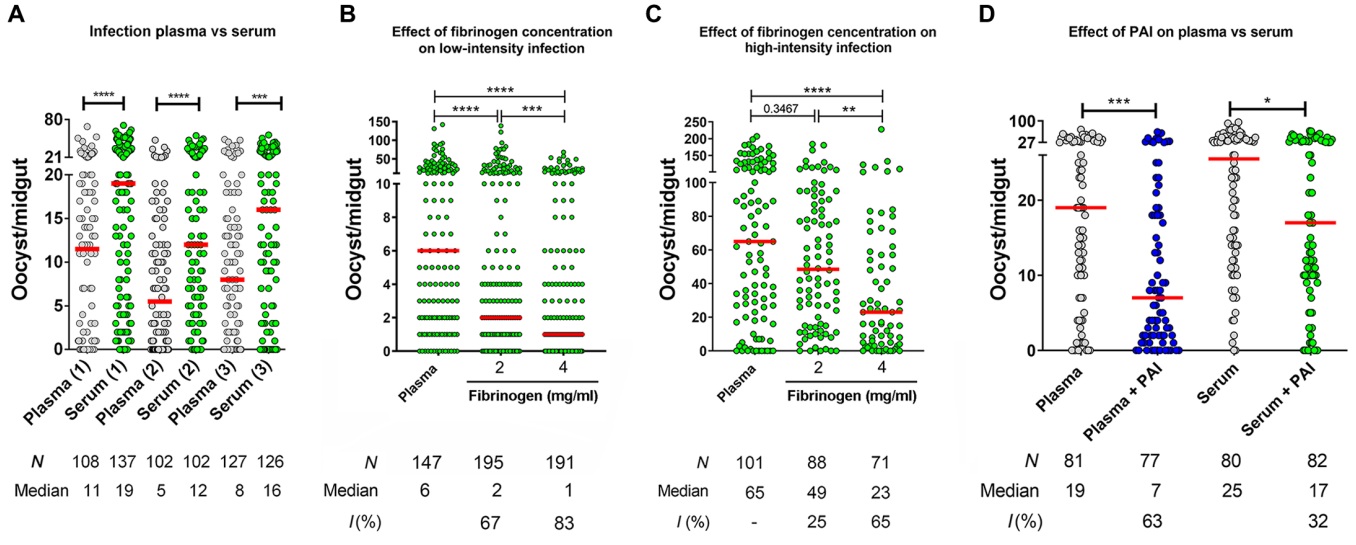

Fig. 4. The concentration of fibrinogen in plasma and serum inversely correlates with *P. falciparum* oocyst formation. (**A**) Effect of plasma versus serum on infection. *P. falciparum* gametocytes fed to mosquitoes in plasma produce fewer oocysts when compared to feeding in serum. Each plasma-serum pair (1-3) was isolated from the same person. Data from each plasma-serum pair pooled from three independent experiments. (**B** and **C**) Increased concentrations of fibrinogen in plasma reduce mosquito infection as measured by oocyst formation on low-intensity (B) and high-intensity (C) infections. Gametocytes were suspended in plasma supplemented with different concentrations of fibrinogen. Data pooled from four (B) and two (C) independent experiments. (**D**) Effect on infection of PAI addition to plasma versus serum. PAI-1 inhibits oocyst development more strongly when the infective meal is in plasma compared to serum. Data pooled from two independent experiments. Dots: Number of oocysts in individual mosquitoes; horizontal red line, median; *N*, number of midguts; *I* (%), percentage inhibition. Mann-Whitney test (A) and Kruskal-Wallis followed by Dunn's multiple comparison posttest (B and D). $*P < 0.05$, $**P < 0.01$, $***P < 0.001$, $****P < 0.0001$.

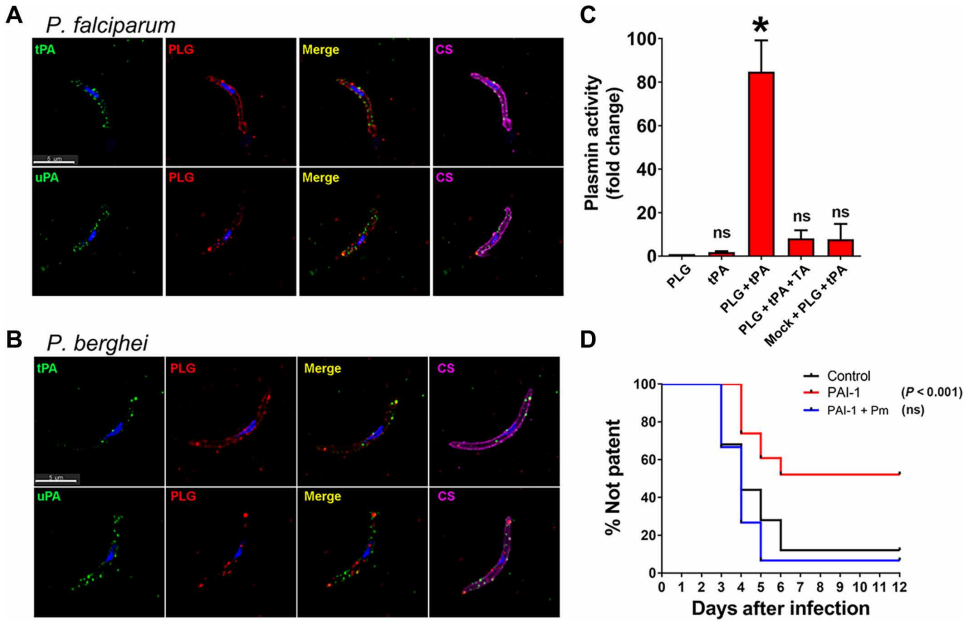

Fig. 5. Plasminogen activation is required for sporozoite infectivity. (**A** and **B**) IFA showing plasminogen (PLG), tPA, and uPA binding to nonpermeabilized *P. falciparum* (A) or *P. berghei* (B) salivary gland sporozoites after incubation with plasma. CS, circumsporozoite protein positive control. (**C**) Plasmin activity on the sporozoite surface was measured after incubation with plasminogen alone, with tPA alone or with plasminogen plus tPA. Preincubation of tPA with tranexamic acid abolished plasmin activation. Mock isolation of noninfected salivary glands was used as negative control. Error bars represent SEM from three independent experiments, $^*P = 0.027$. Plg, plasminogen; mock, preparation from noninfected salivary glands. (**D**) Sporozoite infectivity after infectious mosquito bite was determined in naïve mice injected intravenously with PBS buffer (control), mouse PAI-1, or mouse PAI-1 + plasmin (Pm). Sporozoite infectivity was determined by the day of appearance of blood-stage parasites in peripheral blood (patency). Data pooled from five independent experiments. ($N = 15$ mice or more per treatment). Statistical analysis: log-rank (Mantel-Cox) test with Bonferroni multiple comparison.

passage into the liver or both. To determine whether plasminogen activation influences sporozoite exit from the skin, we intradermally injected sporozoites mixed with PAI-1 (PAI-1 acts locally at the injection site) and/or plasmin into the mouse ear pinna and monitored infection. Inhibition of plasminogen activation at the injection site resulted in 12% protection from blood stage infection and a 1-day delay in patency (Fig. 6A). This inhibition was reverted by coinjection of sporozoites mixed with PAI-1 and plasmin (Fig. 6A). Injection of the same sporozoites/PAI-1 mixture directly into the bloodstream (125 ng of PAI-1 in circulation that represents a 400-fold dilution of PAI-1 in the blood) had no effect on the infection, indicating that PAI-1 does not affect sporozoite viability (Fig. 6A). These results suggest that plasminogen activation is involved in sporozoite exit from the dermal inoculation site.

Plasmodium sporozoites must move through the dermal extracellular matrix to find and enter blood vessels (*3*, *37*). We hypothesized that sporozoites use surface-associated plasmin to degrade extracellular matrix proteins and facilitate movement through host tissues. First, we tested whether PAI-1 has an impact on sporozoite motility on glass slides, where they move in two dimensions and do not encounter extracellular matrix. As shown in Fig. 6 (B and C), PAI-1 has no effect on sporozoite motility in this context. Next, we quantified gliding motility in Matrigel, a reconstituted basement membrane that contains fibrinolytic proteins (*38*). In this context, PAI-1 significantly reduced sporozoite speed and distance traveled, and inhibition was partially reversed by addition of excess active tc-TPA to competitively reverse the PAI-1 inhibition (Fig. 6, D and E, and movies S1 to S3). To confirm the results from the in vitro Matrigel assay, we investigated whether plasmin is important for sporozoite migration in vivo. This was done by using intravital confocal microscopy of fluorescent mCherry *P. berghei* sporozoites injected into the dermis of mice ear pinna, either in the presence or absence of PAI-1. As shown, PAI-1 significantly inhibits sporozoite speed and net displacement in the dermis (Fig. 6, F and G, fig. S8, and movies S4 to S6). Plasmin inhibition of motility in vivo was rescued by coinjection of plasmin (Fig. 6, F and G, fig. S8, and movies S4 to S6). Together, these results indicate that plasminogen activation facilitates sporozoite migration through the extracellular matrix of the dermis.

Plasmin promotes sporozoite liver infection

To determine whether plasminogen activation also plays a role in liver infection, mice were injected intravenously with PAI-1 (50 μg; ~25 ng/μl in circulation) and then challenged by intravenous injection of sporozoites. Intravenous injection of sporozoites bypasses the skin barrier allowing for independent evaluation of liver infection. Mice treated with PAI-1 show 55% protection from blood stage infection and a delay of 1.3 days in patency (Fig. 7A). Coinjection of sporozoites with plasmin reverses the PAI-1 protection (Fig. 7A). In in vitro assays, the presence of PAI-1 or depletion of plasminogen does not affect *P. berghei* sporozoite invasion of Hepa 1-6 hepatocytes (Fig. 7B) nor development of exoerythrocytic forms (EEFs) (Fig. 7C and fig. S9A). Likewise, PAI-1 does not affect *P. falciparum* sporozoite invasion of primary human hepatocytes (PHHs) and EEF development in vitro (Fig. 7D and fig. S9, A and B). We conclude that plasminogen activation is required for liver infection

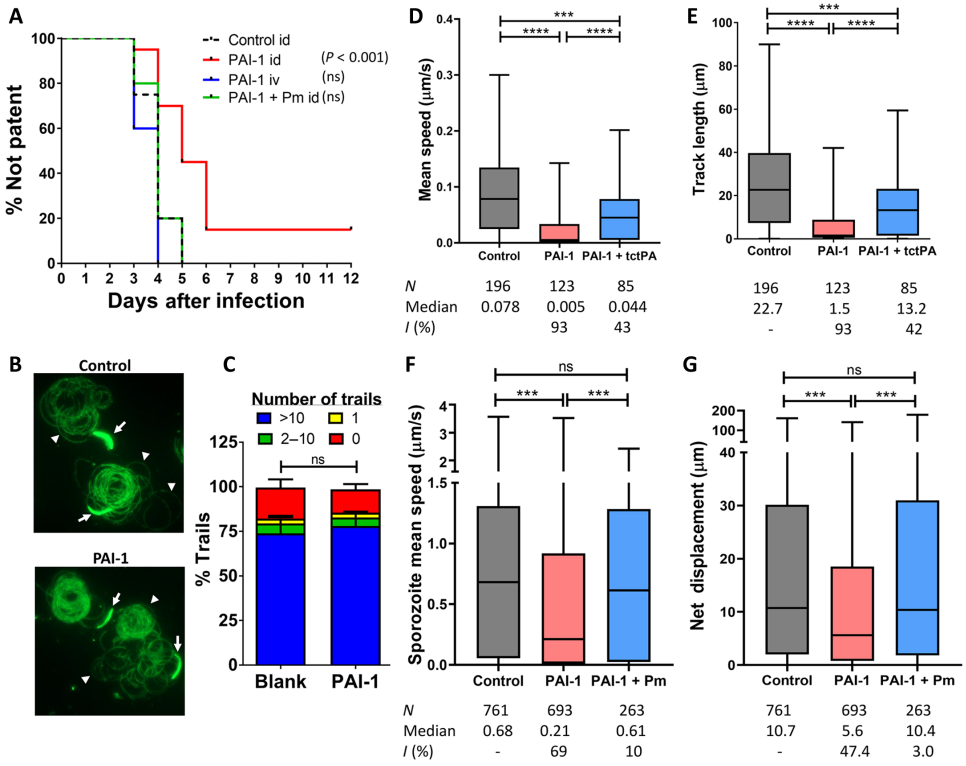

Fig. 6. Plasminogen activation is important for sporozoite migration in the skin. (**A**) Prepatency was determined in mice injected intradermally (id) with sporozoites mixed with PBS, mouse PAI-1, or mouse PAI-1 + plasmin (Pm). Sporozoites mixed with PAI-1 were also injected intravenously (iv) to demonstrate sporozoite viability. Note that after intravenous injection, the PAI-1 (125 ng) becomes diluted approximately 400-fold in the mouse circulation, compared to the intravenous PAI-1 injection experiment of Fig. 7A. Data pooled from three independent experiments. ($N = 15$ mice or more per treatment, except for sporozoite/PAI-1 intravenous where $N = 5$). Statistical analysis: log-rank (Mantel-Cox) test with Bonferroni multiple comparison. (**B**) Sporozoite motility on glass slides determined by the number of circumsporozoite protein (CSP) trails (green circles indicated by white arrowheads) detected by IFA with anti-CSP monoclonal antibody (mAb) 3D11. White arrows point to sporozoites. (**C**) Quantification of CSP trails from (B). Data pooled from two independent experiments. Control: Sporozoites in culture medium. (**D** and **E**) Sporozoite motility was determined in Matrigel mixed with PBS (control) ± PAI-1 or PAI-1 + active tc-tPA. Sporozoite speed (D) and track length (E) were used as determinants of parasite motility. *N*, number of sporozoites assayed. *I* (%), percent inhibition. Data pooled from three independent experiments. (**F** and **G**) mCherry sporozoite speed (F) and net displacement (G) were determined by intravital confocal microscopy of mouse dermis after intradermal injection of sporozoites in PBS, with mouse PAI-1 or with mouse PAI-1 plus plasmin. *N*, number of sporozoites assayed. *I* (%), percent inhibition. Pooled data from five independent experiments. Statistical analysis for (D) to (G): Kruskal-Wallis followed by Dunn's multiple comparison posttest ****$P < 0.0001$, ***$P = 0.0009$.

but not for hepatocyte invasion nor for EEF development in tissue culture.

To reach the hepatocyte, the sporozoite must exit the circulation by traversing Kupffer cells or endothelial cells that line the hepatic blood vessels and then cross the interstitial extracellular matrix and the loose basal lamina of the space of Disse (fig. S1B). To determine whether plasmin is important for parasite migration into the liver, we injected sporozoites intravenously into mice that had been injected intravenously with PAI-1 or PBS. Mouse livers were collected at 3 hours after inoculation, sectioned, and stained for immunofluorescence confocal microscopy to localize parasites within the tissue. Each sporozoite was classified as "outside" if it was associated with any compartment (i.e., Kupffer cells and space of Disse) but not with hepatocytes, in "transition" if a sporozoite had partially invaded a hepatocyte, and"inside" if the sporozoite had fully invaded the hepatocyte (Fig. 7, E and E′, and fig. S9C). In the control group, 75% of sporozoites fully invaded hepatocytes, while the majority of the sporozoites from the PAI-1–treated mice were either outside (32%) or in transition (35%) (Fig. 7F), suggesting an impairment of sporozoite migration into the liver tissue. Coinjection of plasmin and sporozoites rescued the phenotype (72% inside, 16% outside, and 12% transition) (Fig. 7F). These results suggest that the sporozoite uses the surface-associated plasmin to facilitate liver infection.

DISCUSSION

While developing in the mosquito and vertebrate hosts, *Plasmodium* parasites face physical constraints in the form of proteinaceous matrices that they must migrate across. Our results reveal that gametes and sporozoites use a common strategy, namely, they co-opt fibrinolytic proteins from the mammalian host to facilitate motility throughout these barriers. Plasmin, the effector protease of the fibrinolytic system, digests a broad range of substrates including fibrinogen, fibrin, complement proteins, antibodies, and extracellular matrices such as collagen, fibronectin, and laminin (*10*, *11*, *39*). Hence, several pathogens have evolved to co-opt plasmin to infect host tissues (*40*, *41*). Previously, our group showed that *P. falciparum* ookinetes bind plasminogen from the blood ingested by the mosquito (*18*). However, how plasminogen is converted to active plasmin, the role

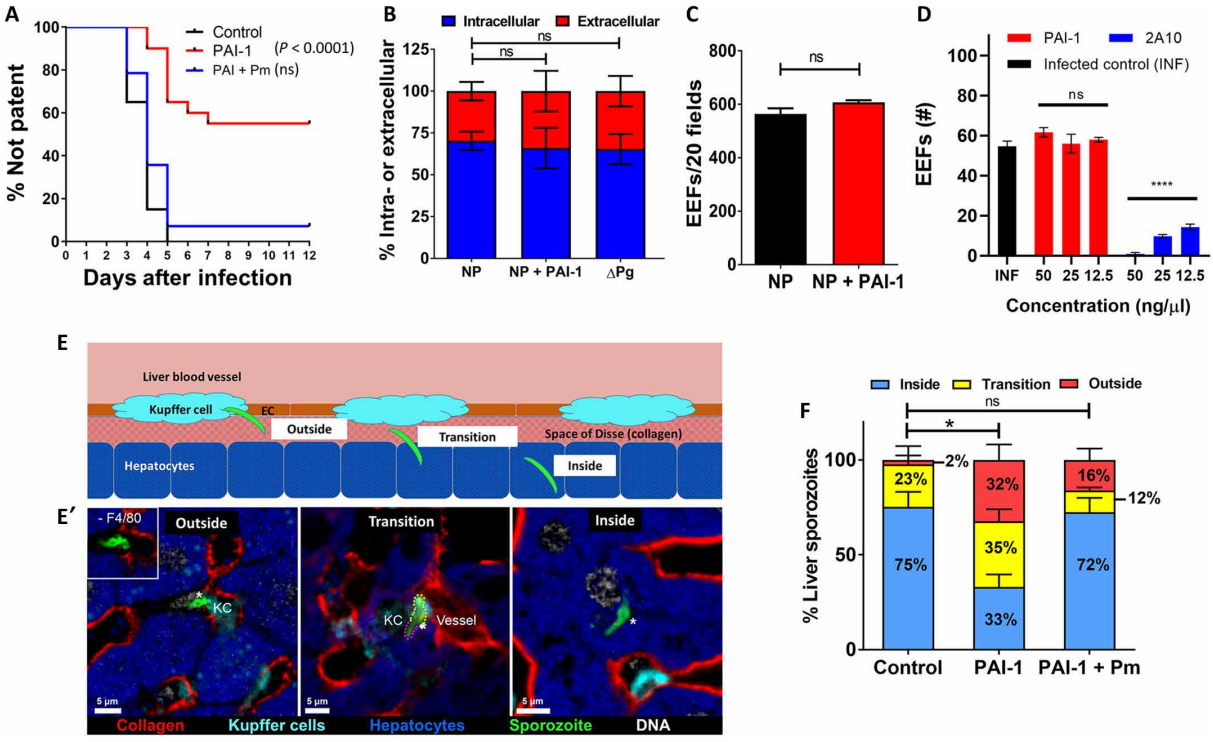

Fig. 7. Plasminogen activation facilitates *P. berghei* sporozoite liver infection. (**A**) Mouse infection was determined after intravenous injection with mouse PAI-1 or PBS, followed by intravenous injection of sporozoites ± plasmin (Pm). Data from four independent experiments ($N \geq 15$ mice per treatment). Statistical analysis: log-rank (Mantel-Cox) test with Bonferroni multiple comparison. (**B** and **C**) *P. berghei* sporozoite invasion and EEF formation in mouse Hepa 1-6 cells in normal plasma (NP), NP + PAI-1, or in plasminogen-depleted plasma (ΔPg). Data from three independent experiments. (**D**) *P. falciparum* EEF quantification (by parasite morphology; fig. S9A) in PHHs incubated with PAI-1 or anti-CSP mAb 2A10 (positive control). Data from two independent experiments, with three experimental replicates. Statistical analysis: One-way ANOVA with Dunnett's multiple comparisons to infected control (INF), ****$P < 0.0001$. (**E** and **E′**) Sporozoite (green) locations during liver invasion. "Outside": Sporozoites with no contact with hepatocytes. "Transition": Sporozoites within hepatocytes (magenta dotted line) and in the space of Disse (collagen IV) and/or Kupffer cells (KC; stained with F4/80) (yellow dotted line). "Inside": Sporozoites that completed invasion. Sporozoites were visualized with anti-CSP, nuclei with JOJO-1 (DNA dye), and hepatocytes with autofluorescence. Representative images of five independent experiments with ≥50 images per phenotype. (**F**) Quantification of the sporozoite localization phenotypes shown in (E and E′) in mice treated intravenously with PBS (control), PAI-1, or PAI-1 + plasmin. Statistical analysis: Dunnett's test, *$P = 0.01$.

of plasmin during parasite development in the mosquito, and a possible role in infection of the mammalian host remained unknown. In this study, we show that both, parasite sexual stages in the mosquito and sporozoites in the mammal, recruit to their surface plasminogen and the tPA and uPA activators. The importance of generating active plasmin is supported by the finding that inhibition of plasminogen activation with the specific PAI-1 serpin results in a strong reduction in ookinete formation and sporozoite infection of the mammalian host.

Using two complementary strategies, chemical inhibition with tPA and uPA inhibitors and physical inhibition using tPA-depleted plasma and anti-uPA antibodies, we demonstrate that inhibition of plasminogen activators significantly reduces midgut infection. We also found that tPA, as well as plasminogen, binds to the surface of gametes, zygotes, and ookinetes, whereas uPA binds to zygotes and male microgametes. The colocalization of plasminogen activators and plasminogen is critical for plasminogen activation (*42*). The tPA and uPA zymogens have low intrinsic activity and are ineffective to activate plasminogen when the activators and plasminogen are circulating in the blood (*43*, *44*). The colocalization of the plasminogen activators and plasminogen increases their local concentration, promoting the activation of plasminogen in a positive loop (*44*, *45*). We show that the reduction in oocyst numbers by plasminogen depletion previously reported (*18*) is due to a reduction in ookinete formation. This reduction in the presence of PAI is not observed in in vitro cultures, as formation of fibrin polymers is inhibited by strong anticoagulants (heparin), and fibrinogen is sharply diluted by the added culture media. Under these conditions, the microgamete can freely move through the culture without the aid of plasmin.

During blood feeding, *Anopheles gambiae* excretes large amounts of fluid to increase the concentration of proteins and RBCs in the bolus. Fibrinogen, one of the most abundant proteins in the blood, interacts with the surface of RBCs, activated platelets, and leukocytes, resulting in cell aggregation. We found that increased fibrinogen concentration and fibrin formation promote RBC aggregation and increase viscosity of the midgut blood bolus, resulting in the inhibition of *P. falciparum* mosquito infectivity. Mosquito saliva contains strong anticoagulants and antiplatelet molecules that facilitate blood feeding by inhibiting clot formation and platelet aggregation (*46*). It is unknown to what extent proteins from saliva inhibit fibrin polymerization in the midgut blood bolus. Since fibrin polymerization takes place in the mosquito blood meal and fibrin affects parasite viability, it is relevant to understand the interplay between the anticoagulants in the mosquito saliva and the activation of the blood

coagulation cascade. Lester and Lloyd (*47*) reported that, although tsetse flies with removed salivary glands could feed normally, they died later with clots found throughout the alimentary canal. After the mosquito ingests infected blood, male and female *Plasmodium* gametocytes and gametes are randomly dispersed in the blood bolus. Since fibrinogen and fibrin are natural substrates for plasmin, we propose that plasmin on the surface of male microgametes digests fibrin, in this way facilitating motility in the compacted blood bolus and increasing its chances to encounter a female gamete. Also, plasmin on the surface of female gametes may degrade fibrin polymerized on the gamete's surface, minimizing a barrier for gamete interaction.

A question that remains to be addressed is whether later midgut stages, such as zygotes and motile ookinetes, benefit from plasmin activity, as these forms also bind plasminogen and its activator enzymes. It is possible that zygotes use plasmin to inactivate blood complement that remains active for hours after blood feeding (*48*). Plasmin may inactivate complement directly by digestion of C3b (*49*) or indirectly by activating protease factor I, which, in turn, inactivates C3b. In addition, activated platelets present in the blood bolus, which are absent in our assays, potentially enhance complement activation and fibrin formation (*50*). Moreover, ookinetes may use plasmin activity to facilitate the crossing of midgut barriers, including the peritrophic matrix (fig. S1A) and the microvilli-associated network, a mesh of fine proteinaceous strands associated with the microvilli (*6*, *51*). Additional experiments are required to show whether plasmin facilitates ookinete traversal of the mosquito midgut, as previously suggested (*18*).

Like the midgut stages, we found that sporozoites also bind plasminogen, tPA, and uPA and that inhibition of plasminogen activation by PAI-1 inhibits *P. berghei* sporozoite infectivity. Successful infection depends on the effective migration of sporozoites from the dermis (where they are deposited by the mosquito) to a blood vessel and then migration through the space of Disse as they leave the liver circulation (fig. S1B). During this trajectory, the sporozoites encounter physical barriers such as the extracellular matrix of the dermis, the basal lamina of blood vessels, the sinusoidal barrier of Kupffer and endothelial cells, and the extracellular matrix of the space of Disse (*52*). While it is known that sporozoites rely on an actomyosin-based motor known as the glideosome (*8*) to drive motility, it was not clear by what mechanisms the parasite overcomes these physical barriers. Inhibition of plasminogen activation reduces parasite motility on Matrigel, in the mouse dermis and in the mouse liver, strongly suggesting that the parasites use plasmin for overcoming these barriers. PAI-1 does not affect sporozoite motility on a glass surface, showing that the gliding locomotion machinery is not affected. In addition, invasion of cultured hepatocytes, which does not require traversal of the extracellular matrix of the space of Disse, and EEF development are also not affected by PAI-1. Sporozoites can traverse several hepatocytes before completing a productive invasion that results in the formation of EEFs (*53*). Our data suggest that sporozoite productive invasion of hepatocytes is independent of plasmin. However, our in vitro assays do not measure cell traversal, and additional experiments are needed to determine whether plasmin is required for sporozoite traversal of hepatocytes. Recruitment of plasmin for penetration of extracellular matrices is a mechanism used by several pathogens to enhance invasion and dissemination through target organs (*41*, *54*). For example, *Borrelia burgdorferi*, *Haemophilus influenzae*, and *Salmonella* can degrade extracellular matrix components like fibronectin, laminin, and vitronectin (*55*–*57*). Degradation of the extracellular matrix can be directly mediated by plasmin or indirectly by plasmin activation of matrix metalloproteases (MMPs) (*58*–*61*). In the case of *Plasmodium*, whether degradation of the extracellular matrix is direct by plasmin, indirect via MMPs, or involve both classes of proteases remains to be determined.

In summary, our results provide mechanistic insights into how *Plasmodium* parasites co-opt the human fibrinolytic system to support its development in the vector and in the mammalian host, opening the possibility of targeting these interactions for malaria transmission-blocking interventions. One strategy is the use of available antifibrinolytic drugs like aprotinin, ε-aminocaproic acid, and tranexamic acid, currently used during surgeries of patients with high risk of bleeding (*62*). However, this strategy is not feasible to control malaria transmission as the drugs will have to be constantly administered over an extended period, which will alter the fibrinolytic homeostasis. Another alternative is to identify the parasite's receptors for tPA, uPA, and plasminogen, as these receptors are potential targets for transmission-blocking interventions (*18*). In addition, innovative strategies including transgenic mosquitoes (*63*) or transgenic mosquito symbionts (paratransgenesis) (*64*, *65*), producing molecules that prevent the parasite from using the fibrinolytic proteins are currently being developed.

MATERIALS AND METHODS

Experimental design

The objective of this study was to establish the mechanism by which the mammalian fibrinolytic system, as well as its central protease plasmin, promotes *Plasmodium* infection of the mosquito vector and the vertebrate host. A previous study showed that *Plasmodium* requires plasmin for infection of the mosquito. We hypothesized that the parasite uses the plasmin protease activity to degrade fibrin and extracellular matrix proteins, thereby facilitating parasite migration in the mosquito blood bolus and in the extracellular matrices of the vertebrate skin and liver. For experiments with *P. falciparum*, we used in vitro–cultured parasites and standard membrane feeding assays to determine the effect of treatment on parasite development in *An. gambiae* mosquitoes. To assess the role of plasmin during sporozoite infection of the mammalian host, we used a combination of in vitro and in vivo experiments in mice. Group sizes were determined on the basis of previous publications. Most experiments were performed at least in triplicate. Sodium citrate was used as anticoagulant for human plasma collection.

Animal ethics protocol

The study was performed in strict accordance with the recommendations from the Guide for Care and Use of Laboratory Animals of the National Institutes of Health (NIH). The animal use was done in accordance with protocol MO18H18 approved by the Johns Hopkins University Animal Care and with the Use Committee or The NIH Animal Ethics Proposal SOP LMVR 22.

Parasite and mosquito strains

An. gambiae (Keele) (*66*) or *Anopheles stephensi* (Nijmegen) (*67*) mosquitoes were reared at 27°C and 80% humidity with a 14-hour/10-hour light/dark cycle under standard laboratory conditions. *P. falciparum* NF-54 gametocyte cultures were provided by the Johns Hopkins Malaria Research Institute Parasite Core Facility.

Mosquito infections

Mosquitoes were infected by membrane feeding with reconstituted human blood. Briefly, a suspension of human RBCs was mixed with human plasma (Innovative Research) at 50% hematocrit. The infected blood was diluted to 0.05% gametocytemia before feeding to the mosquitoes. When specified, the blood was reconstituted with tPA-depleted human plasma (Innovative Research) or supplemented with human sc-tPA (Innovative Research) at 5, 50, and 500 ng/μl. To inhibit uPA activity, reconstituted blood was supplemented with the uPA inhibitor DGGACK (EMP-Millipore) at 0.5, 5, and 50 μM. To inhibit both, tPA and uPA, the normal plasma-reconstituted blood was supplemented with different concentrations of PAI-1 (Innovative Research). To rescue PAI-1 inhibition, the PAI-1–treated blood was supplemented with plasmin (Sigma-Aldrich) at 100 and 200 μg/ml. Plasma controls were supplemented with a volume of PBS equivalent to the volume of treatments. To estimate oocyst numbers, midguts were dissected in PBS 10 days after infection, stained with 0.2% mercurochrome, and mature oocysts were counted with a dissecting microscope.

To determine the impact of PAI-1 on fertilization, mosquitoes were fed with blood containing 0.2% gametocytemia in the presence or absence of 2.5 μg/ml of PAI-1. Plasma controls were supplemented with a volume of PBS equivalent to the volume of treatments. Individual midguts were dissected 22 to 23 hours after feeding, homogenized in 50 μl of PBS, and 5 μl of this suspension was smeared and immunostained using anti-Pfs25 antibody (see the "Immunofluorescence assay" section below). To test the impact of different concentrations of fibrinogen on plasma, we fed *An. gambiae* females with infected RBCs (*P. falciparum* NF54, gametocytemia 0.08% or 1.5%) diluted to 50% hematocrit with control normal plasma or control plasma plus Fibrinogen (2 or 4 mg/ml) (Sigma-Aldrich). Oocyst numbers were counted 10 days after infection. In addition, infections were tested using plasma or serum isolated from three volunteers. Serum was supplemented with 3.2% sodium citrate, the same concentration used to isolate the plasma. Under a Johns Hopkins Medicine Institutional Review Board–approved protocol, blood from healthy volunteers is procured weekly and provided without identifiers to qualified investigators to culture malaria parasites in vitro, propagate the mosquito vectors of malaria, or infect mosquitoes with malaria. Volunteers reviewed and signed a written informed consent.

The effect of fibrinogen on infections performed with Albumax, a solution of Albumax composed of 5% (w/v) Albumax II (Gibco, Life Technologies) in RPMI 1640 (Gibco, Life Technologies), with addition of L-glutamine and 25 mM Hepes (Corning Cellgro) was supplemented with fibrinogen (4 mg/ml) or fibrinogen plus plasmin (100 ng/ml) (Sigma-Aldrich). Infections were performed at 0.05% gametocytemia.

In vitro *P. berghei* ookinete differentiation

P. berghei ookinete in vitro cultures were performed as previously described (*68*). Briefly, mice were injected intraperitoneally with a solution of 200 μl phenylhydrazine (10 mg/ml)/1× PBS (Sigma-Aldrich). Three days later, mice were infected intraperitoneally with 10^8 *P. berghei*–GFP infected RBCs. Three days later, the gametocyte-enriched blood was collected by cardiac puncture and cultured in 96-well plates with ookinete culture medium containing PAI-1 (2.5 μg/ml) or an equal volume of PBS, for 24 hours at 19°C with gentle agitation. Parasites were fixed with 4% (w/v) paraformaldehyde and stained with an anti-Pbs21 antibody (*69*). Parasites were counted under a fluorescence microscope, and ookinete differentiation was determined as the percentage ookinetes (banana-shaped Pbs21-positive cells) from the total number of Pbs21-positive parasites (ookinetes plus round-shaped gametes and zygotes). Parasites micrographs were taken on Leica SP8 DMI 6000 confocal microscope (Leica Microsystems, Wetzlar, Germany) with 63× oil immersion objective and using a zoom factor of 4. equipped with a photomultiplier tube/hybrid detector. Samples were visualized with a white light laser, and specific emission and excitation range were used depending on the fluorophore used. Images were taken using sequential acquisition and variable z-steps. Image processing was performed using Imaris 9.2.1 (Bitplane, Concord, MA, USA).

Tc-tPA activity

The enzyme tc-tPA (100 nM, Innovative Reseach) was incubated with PAI (100, 250, or 500 nM) in 0.01% Tween 20, tris-buffered saline (TBST) [50 mM tris-Cl (pH 7.5) and 150 mM NaCl] for 15 min at room temperature. The fluorogenic substrate D-Val-Leu-Lys 7-amido-4-MC (10 μM) (Sigma-Aldrich) was added, and the change in fluorescence (excitation, 280; emission, 460) was recorded every 5 min over a period of 2 hours at 37°C. Fluorescence was measured using the Cytation 5 microplate reader (BioTek Instruments, USA).

Heme quantification on blood fed mosquitoes

Mosquito were allowed to feed by standard membrane feeding assay on RBCs resuspended in plasma, plasma plus PAI-1 (250 ng/ml), or plasma plus PAI-1 and plasmin (200 μg/ml). Midguts were dissected 30 min after blood feeding and each midgut was individually homogenized in 1 ml of water. Midguts from unfed females (non-bf) were used as negative control. The spectra (300 to 600 nm) of each individual replicate was then measured in a Cytation 5 Cell Imaging Multi-Mode Reader (BioTek Instruments, USA) and recorded with the Gen5 Image Prime software version 3.04. (BioTek Instruments, USA). Protein-bound heme was measured at 410 nm (*70*).

Immunofluorescence assays

P. falciparum gametes were obtained from gametocyte cultures after activation for 20 min in RPMI 1640 supplemented with 10% (v/v) plasma and 100 μM xanthurenic acid. Zygotes and ookinetes were obtained from midguts dissected at 4 and 19 hours after blood feeding, respectively. Briefly, midguts were homogenized in PBS, and the cell suspension was washed twice with the same buffer. For microscopy, parasites were allowed to sediment onto poly-lysine-coated coverslips (Sigma-Aldrich) for 15 min and fixed for 20 min in PBS containing 4% (w/v) paraformaldehyde and 0.01% (v/v) glutaraldehyde (Sigma-Aldrich); the slides were then washed three times with PBS. The samples were blocked in 5% (w/v) BSA and 0.1% (w/v) gelatin in PBS (blocking buffer) for 1 hour. For double staining, the slides were incubated for at least 2 hours with different combinations of antibodies: rabbit anti-human plasminogen (1:1000, Abcam) and sheep anti-human tPA (5 μg/ml, Innovative Research); rabbit anti-human uPA (5 μg/ml, Innovative Research) and sheep anti-human plasminogen (5 μg/ml, Innovative Research); and sheep anti-human tPA (5 μg/ml, Innovative Research). The samples were washed, blocked for 1 hour, and incubated with secondary antibodies conjugated to either Alexa Fluor 488 (green) or Alexa Fluor 594 (red) dyes (1:2500) (Thermo Fisher Scientific) for at least 2 hours. The coverslips were mounted with ProLong Gold antifade reagent with 4′,6-diamidino-2-phenylindole

(DAPI) (Invitrogen), and images were viewed with a Nikon Plan Apo 100×/numerical aperture (NA) 1.4 objective and a Hamamatsu GRCA-ER camera (Hamamatsu Photonics, Hamamatsu, Japan) using a Nikon Eclipse 90i microscope (Nikon Instruments Inc.). Optical z-sections with 0.2-μm spacing were acquired using Volocity software version 6.3 (PerkinElmer). Images were processed by deconvolution using iterative restoration (confidence limit 100% and iteration limit 25). Adobe Photoshop software (Adobe, San Jose, CA) was used to adjust levels, crop, and resize images.

For quantification of tPA, uPA, and plasminogen binding, gametes (activated in vitro as described above) and zygotes (from mosquito midguts) were activated in the presence of aminocaproic acid (400 μg/ml, Sigma-Aldrich) or tranexamic acid (400 μg/ml, Sigma-Aldrich), respectively. The parasites were immunostained as described above using anti-tPA, anti-uPA, or anti-plasminogen antibodies. Cell-associated fluorescence was quantified by substracting the background relative fluorescence using ImageJ software (NIH, USA).

Salivary gland sporozoites were obtained by dissecting *An. stephensi* salivary glands 21 days after feeding on *P. berghei*–infected mice or 21 days after feeding on *P. falciparum* gametocytes. The salivary glands were homogenized using a blue plastic pestle, and the free sporozoites were either incubated with 5% plasma or with PBS as negative control for 20 min at 37°C. Sporozoites were centrifuged against a poly-L-lysine–coated coverslips at 300*g* for 4 min. Coverslips were washed three times with PBS, and sporozoites were fixed with a PBS solution containing 4% (w/v) paraformaldehyde for 20 min at room temperature. The coverslips were washed three times with PBS and blocked for 1 hour at room temperature with 2% (w/v) BSA in PBS (blocking buffer). The samples were stained for 1 hour at room temperature with either a combination of sheep anti-human plasminogen (5 μg/ml, Innovative Research) and rabbit anti-human uPA (5 μg/ml, Innovative Research) or sheep anti-human tPA (5 μg/ml, Innovative Research) and rabbit anti-human uPA (5 μg/ml, Innovative Research) diluted in blocking buffer. After three washes with PBS, the coverslips were incubated with secondary antibodies conjugated to Alexa Fluor 488 (1:2500) for 1 hour. After three washes with PBS, the coverslips were mounted with ProLong Gold antifade reagent with DAPI (Invitrogen), and images were viewed with a Nikon Plan Apo 100×/NA 1.4 objective and a Hamamatsu GRCA-ER camera (Hamamatsu Photonics, Hamamatsu, Japan) using a Nikon Eclipse 90i microscope (Nikon Instruments Inc.). Optical z-sections with 0.2-μm spacing were acquired using Volocity software version 6.3 (PerkinElmer). Images were processed using iterative restoration (confidence limit, 100%; iteration limit, 25). Alternatively, sporozoites were imaged using a Leica TCS SP8 DMI 6000 confocal microscope (Leica Microsystems, Wetzlar, Germany) as described above.

Confocal microscopy of liver invasion: Mice were injected intravenously with either 100 μl of PBS (group 1, control) or mouse recombinant PAI-1 (0.5 μg/μl; stable mutant, Innovative Research) (groups 2 and 3). After 1 hour., 300,000 *P. berghei* salivary gland sporozoites were injected intravenously into PBS-injected mice ($n = 5$ per experiment) and into half of the PAI-injected mice (group 2, $n = 5$ per experiment). The other half of PAI-1–injected mice ($n = 5$ per experiment) were injected intravenously with sporozoites mixed with human plasmin (100 μg) (Sigma-Aldrich). After 3 hours, livers were perfused with 20 ml of periodate-lysine-paraformaldehyde (PLP) buffer {37% P-buffer [P-buffer = 8.1 mM Na_2HPO_4 and 1.9 mM NaH_2PO_4 (pH 7.4)], 9.9 mM $NaIO_4$, 75.0 mM L-lysine, and 2% paraformaldehyde}. Perfused livers were dissected and fixed overnight at 4°C in PLP buffer, washed twice in P-buffer, and incubated overnight at 4°C in 30% sucrose. Fixed livers were mounted in optimal cutting temperature compound (Tissue-TEK) and cut in a microtome (30 μm). Slices were mounted on Super Frost Plus Gold slides (Electron Microscopy Services), permeabilized, and blocked overnight at 4°C with PBS containing 0.3% Triton X-100, 1% BSA, and 1% murine Fc seroblock (clone 2.4G2; BD Biosciences). Sections were stained with the following primary antibodies: anti-F4/80 monoclonal antibody (mAb) (clone BM8; BioLegend), anti-collagen IV (polyclonal rabbit; Abcam), and anti–circumsporozoite protein (CSP) mAb (clone 3D11) (*71*). Slides were washed three times with 0.2% Triton X-100 in PBS for 1 hour per wash, at room temperature on a shaker. Samples were stained overnight at 4°C with the secondary antibody anti-rabbit immunoglobulin G (IgG) Alexa Fluor 700 (Thermo Fisher Scientific). Slides were washed three times with 0.2% Triton X-100 in PBS for 1 hour per wash, at room temperature on a shaker. Slides were mounted with Fluoromount G (eBiosciences) and sealed with a glass coverslip. Representative images of sections from different livers were acquired with a SP8 confocal microscope (Leica) equipped with a 40× objective (NA 1.3). Hepatocytes were visualized by their autofluorescence using the 405 laser with detector at 510 to 550, and cell nuclei were visualized with JOJO-1 (Thermo Fisher Scientific).

Cell surface plasminogen activation

The activation of female gametes was performed as described above, except that human serum was substituted with Albumax. Gametes were purified using a density gradient as described previously (*72*). The parasites were suspended at 2×10^6 cells/ml and incubated for 1 hour in PBS containing sc-tPA (100 ng/ml) (Innovative Research). Cells were washed three times with PBS and incubated in PBS containing plasminogen (100 μg/ml) for 1 hour. Following washing, cell surface plasmin activity was measured using the specific plasmin chromogenic substrate (D-Val-Leu-Lys 4-nitroanilide dihydrochloride, Sigma-Aldrich). Plasmin activity was monitored by continuously measuring the rate of change of absorbance at A405 nm. For controls, either or both tPA and plasminogen were omitted. Alternatively, plasminogen was incubated in the presence of tranexamic acid (100 μg/ml).

Sporozoites. *P. berghei* salivary gland sporozoites (100,000) were incubated with human plasminogen for 1 hour at 37°C. Sporozoites were centrifuged at 10,000*g* for 5 min at 4°C and washed twice with PBS. Sporozoites were incubated for 1 hour at 37°C with either sc-tPA (100 ng/ml) or tPA preincubated with 10 mM tranexamic acid. Sporozoites were centrifuged at 10,000*g* for 5 min at 4°C and washed twice with PBS. Sporozoites were incubated only with plasminogen or tPA as negative controls. Noninfected salivary glands were dissected and processed similarly as for sporozoite isolation and were used as "mock preparations." Activation of plasminogen was determined using the SensoLyte AFC Plasmin Activity Assay Fluorimetric Kit (AnaSpec) following the manufacturer's recommendations. Fluorescence readings for plasmin activity were obtained using a Molecular Devices SpectraMax (Molecular Devices) with excitation at 380 nm and emission at 500 nm.

Western blot assays

Blood-fed mosquitoes were dissected 15 min and 1 hour after blood feeding in PBS supplemented with 5 mM EDTA, 0.1 mM phenylmethylsulfonyl fluoride (Sigma-Aldrich), and protease inhibitors (#P8340, Sigma-Aldrich). A total of five midguts were pooled in

50 µl of PBS, then the midguts were macerated on ice, and reducing SDS–polyacrylamide gel electrophoresis (PAGE) sample buffer was added to the samples. A total of 0.25 midgut equivalent was separated by SDS-PAGE and transferred to polyvinylidene difluoride membranes (Millipore). The membrane was blocked with blocking buffer (5% milk powder in TBST) overnight at 4°C following incubation with goat anti-human fibrinogen antibody (1:10,000 in TBST; Sigma-Aldrich). Membranes were incubated with anti-goat horseradish peroxidase (1:30,000 in TBST; Sigma-Aldrich) for 1 hour at room temperature and detected using SuperSignal West Pico PLUS Chemiluminescent Substrate (Thermo Fisher Scientific).

ImageStream flow cytometry

Female mosquitoes were fed on blood reconstituted with plasma, serum, Albumax (Thermo Fisher Scientific), or Albumax plus fibrinogen (4 mg/ml). Individual midguts were dissected 5 min after feeding and disrupted in 50 µl of PBS. The volume was adjusted slowly to 200 µl of PBS, and the samples were immediately analyzed on an Amnis ImageStreamX Mark II flow cytometer (Luminex) with high-resolution imaging capability. Individual images of each event were recorded. The events were gated on the basis of aspect ratio versus area. Images were recorded at ×40 magnification and run at high speed with a 7-µm core size. A total of 10,000 events were analyzed. Data analysis was performed using IDEAS software version 6.0 (Amnis–EMD Millipore).

Prepatency assays

For mosquito challenge: Mice were injected intravenously with 50 µg of mouse PAI-1 stable mutant (Innovative Research), with [50 µg mouse PAI-1 stable mutant (Innovative Research) plus 100 µg of human plasmin (Sigma-Aldrich)], or with PBS. Mice where challeged 30 min later with the bite of three *An. stephensi* mosquitoes infected with *P. berghei* parasites expressing mCherry under the UIS4 promoter (*73*). Infection status of mosquito salivary glands was verified before the challenge by the presence of strong red fluoresnce in the thoracic cavity. Mouse infection patency was monitored by Giemsa-stained blood smears for 12 days after infection. A single experiment included five mice for each treatment.

For intradermal sporozoite challenge: Mice were anesthetized by peritoneal injection of ketamine (50 mg/kg body weight) and xylazine-hydrochloride (10 mg/kg body weight), and then 5000 sporozoites were injected intradermally into the ear in a total volume of 5 µl of PBS, PAI-1 (25 ng/µl), or [PAI-1 (25 ng/µl) plus plasmin (10 µM)]. Mice were maintained on a 37°C warm plate before and 30 min after sporozoite injection. Infection patency was monitored by Giemsa-stained blood smears for 12 days after parasite inoculation. A single experiment included five mice for each treatment.

For intravenous sporozoite challenge: Mice were injected intravenously with either PBS (group 1) or 50 µg of mouse PAI-1 stable mutant (groups 2 and 3). At 1 hour later, mice were injected intravenously with 200 sporozoites (groups 1 and 2) or 200 sporozoites mixed with 100 µg of plasmin (group 3). Infection patency was monitored by Giemsa-stained blood smears for 12 days after parasite inoculation. A single experiment consisted of five mice for each treatment.

Sporozoite motility

Matrigel: *P. berghei* mCherry sporozoites were mixed with an equal volume (5 µl) of Geltrex LDEV-Free Reduced Growth Factor Basement Membrane Matrix (Thermo Fisher Scientific) mixed with buffer, PAI-1 (25 ng/µl), or PAI-1 (25 ng/µl) plus sc-tPA (25 ng/µl). The mixture was applied onto a glass slide, then covered with a round coverslip, and incubated at 37°C for 5 min to allow the matrix to solidify. Sporozoite motility was immediately monitored under a fluorescence microscope for 5 min at room temperature with frames taken every 5 s. Image sequences were manually analyzed with the ImageJ Manual Tracking plugin.

Mouse dermis: Sporozoite motility in the mouse dermis was monitored as previously described (*73*). Briefly, *P. berghei* mCherry sporozoites were injected intradermally in the dorsal side of the ear pinna of anesthetized mice using a 10-µl NanoFil syringe with a NF33BV-2 needle (World Precision Instruments). The ear pinna was taped to a coverslip, and the mouse was mounted on an inverted Zeiss Axio Observer Z1 microscope with a Yokogawa CSU22 spinning disk prewarmed at 30°C. Parasites were visualized using a 10× objective and magnified with a 1.6 Optovar on *Z*-stack containing three sections spanning a total depth of 30 to 50 µm, with a frame rate of 1000 ms per frame using an electron-multiplying charge-coupled device camera (Photometrics, Tucson, AZ, USA) and the 3i SlideBook 5.0 software (Intelligent Imaging Systems). Images were projected into single z-layer, and sporozoite motility was manually tracked using Imaris software (Bitplane, Concord, MA, United States).

Glass slide: Sporozoite motility on glass slides was assessed as previously described (*74*). Briefly, salivary gland sporozoites were dissected in RPMI 1640 containing 3% BSA and added to Lab-Tek wells (20,000 sporozoites per well) previously coated with an anti-CSP mAb 3D11 for 1 hour at 37°C in the presence or absence of mPAI-1 (25 ng/µl). Wells were washed, fixed with 4% w/v paraformaldehyde in PBS, blocked with 1% BSA in PBS, and stained with biotinylated 3D11 anti-CSP antibody. Streptavidin conjugated to Alexa Fluor 488 (Thermo Fisher Scientific) was used to visualize the biotinylated 3D11 antibody binding to the CSP trails shed during sporozoite movement. Sporozoite motility was quantified by the number of trails (circles) associated with each sporozoite.

P. berghei hepatocyte invasion and EEF development

Hepa 1-6 cells were grown in monolayers in Lab-Tek chambers. Each well was seeded with 20,000 sporozoites in the presence or absence of mouse PAI-1 (25 ng/µl). Lab-Tek chambers were centrifuged at 300*g* at room temperature for 4 min to sediment the sporozoites toward the hepatocytes. Sporozoites were allowed to invade the hepatocytes for 1 hour by incubation at 37°C in 5% CO_2. After 3 hours, each well was carefully washed three times with PBS and fixed with 4% paraformaldehyde in PBS overnight at 4°C. For intracellular-extracellular double labeling, we followed a previously published protocol (*75*) with modifications. Wells were washed with buffer, blocked with 1% PBS/BSA, stained with anti-CSP mAb 3D11 for 1 hour at 37°C, and then stained with a goat anti-mouse IgG antibody labeled with Alexa Fluor 488 (Invitrogen) for 1 hour at 37°C. This staining is to visualize extracellular sporozoites. After washing three times, cells were permeabilized with 0.05% Triton X-100/PBS for 20 min at 37°C. Cells were washed, blocked with 1% PBS/BSA, stained with mAb 3D11 for 1 hour at 37°C, and then stained with goat anti-mouse IgG antibody labeled with Alexa Fluor 594 (Invitrogen) for 1 hour at 37°C. After three washes with PBS, the cells were mounted with ProLong Gold Antifade Mountant with DAPI (Invitrogen) for visualization in a fluorescence microscope. Sporozoites were scored as extracellular if they showed green and red fluorescence or intracellular if they showed only red fluorescence.

For EEF development, Hepa 1-6 cells grown in monolayers Lab-Tek chambers were seeded with 20,000 sporozoites in the presence or absence of mouse PAI-1 (25 ng/μl). Lab-Tek chambers were centrifuged at 300*g* at room temperature for 4 min to sediment the sporozoites against the hepatocytes. Sporozoites were allowed to invade the hepatocytes for 2 hours by incubation at 37°C in 5% CO_2. Wells were washed three times with culture media to remove extracellular sporozoites, followed by addition of fresh 400 μl of media with or without mouse PAI-1. Cells were cultured for 48 hours with culture media change every 12 hours (with or without mouse PAI-1). After 48 hours, wells were washed with PBS, fixed with 4% paraformaldehyde in PBS at 4°C overnight, and permeabilized with 100% methanol at −20°C for 20 min. Wells were washed with PBS, blocked with 1% PBS/BSA, and probed with anti-PbHSP70 mAb 2E6 (*76*) for 1 hour at room temperature. Wells were washed with PBS and stained with goat anti-mouse IgG antibody labeled with Alexa Fluor 488 (Invitrogen). After three washes with PBS, the cells were mounted with ProLong Gold Antifade Mountant with DAPI (Invitrogen) for visualization in a fluorescence microscope. Slides were visualized using the 20× objective to score the number of EEFs developing on each field. A total of 100 fields were evaluated for each well.

P. falciparum PHH invasion and EEF development

P. falciparum PHH invasion and EEF development experiments were performed as previously described (*77*). Briefly, cryopreserved PHH (catalog no. M00995-P, donor YNS, BioIVT Inc., Baltimore, MD, USA) were thawed following manufacturer's protocol and diluted in hepatocyte culture medium (HCM) to a concentration of 900 cells/μl (18,000 PHHs per well). The cell mixture was seeded as a confluent monolayer in a commercial 384-well plate (catalog no. 781956, Greiner, Monroe, NC, USA) and 2 days after seed each well received a complete media change. Salivary glands were dissected 15 days after infected blood feed from *P. falciparum*–infected *An. stephensi* mosquitoes and collected into 100 μl of dissection media, followed by gland disruption. Sporozoites were counted using a hemocytometer and diluted to 1000 sporozoites/μl in HCM to a final concentration of 20,000 sporozoites per well. The cryopreserved *P. falciparum* sporozoites used for the second biological replicate were produced and thawed following previously described methodologies (*78*). The mAb clone 2A10 anti–*P. falciparum* CSP, MRA-183A, was obtained through BEI Resources, National Institute of Allergy and Infectious Diseases (NIAID), NIH and used as the assay positive control for blocking of sporozoite invasion. The human PAI-1 and positive control were diluted in HCM and tested at the final concentrations of 50, 25, and 12.5 ng/μl. Collected sporozoites were added to conditioned wells in triplicates and exposed for 24 hours at 37°C before washing with HCM. Medium was changed every 2 days using HCM with 1% penicillin-streptomycin-neomycin until fixation 5 days after infection.

IFA for EEF visualization and quantification: At 5 days after infection, wells were fixed with 4% paraformaldehyde for 20 min at room temperature and washed thrice with PBS. Wells were incubated in blocking buffer (1% BSA and 0.3% Triton X-100 in PBS) with mouse anti–glyceraldehyde 3-phosphate dehydrogenase (3.2 μg/ml at 1:5000-fold dilution), obtained from The European Malaria Reagent Repository (www.malariaresearch.eu) overnight at 4°C. Wells were washed thrice with PBS and incubated for 1 hour at room temperature with secondary goat anti-mouse Alexa Fluor 555 Plus (2 μg/ml at 1:1000-fold dilution) (Thermo Fisher Scientific) and Hoechst 33342 (10 μg/ml at 1:1000-fold dilution) (Thermo Fisher Scientific) and then washed thrice and filled with PBS for imaging and storage.

Imaging and data analysis: High-resolution z-stack IFA images of *P. falciparum* EEFs were captured with a water immersion 63×, 1.75 NA objective on a Operetta CLS Imaging System using Harmony 14.2 software for image processing (Perkin Elmer). Parasite growth was determined by quantification of developing EEFs based on fluorescence intensity and morphology. Statistical significance of parasite growth was determined using one-way analysis of variance (ANOVA) followed by Dunnett's multiple comparisons to the infected control where values are represented by $^{****}P < 0.0001$ and no significance (ns) as defined in Prism (GraphPad, La Jolla, CA, USA).

Statistical analysis

Data were analyzed with GraphPad Prism version 7.04. Data from mosquito infections are not normally distributed and were analyzed with nonparametric Mann-Whitney test or Kruskal-Wallis test with Dunn's multiple comparison posttest. Prepatency assays were analyzed using the log-rank (Mantel-Cox) test with Bonferroni multiple comparison. Data with normal distribution were analyzed with one-way ANOVA with Dunnett's or Tukey's multiple comparison test. *P* values are defined in each figure.

Supplementary materials

Supplementary material for this article is available at http://advances.sciencemag.org/cgi/content/full/7/6/eabe3362/DC1

View/request a protocol for this paper from *Bio-protocol*.

REFERENCES AND NOTES

1. S. Bennink, M. J. Kiesow, G. Pradel, The development of malaria parasites in the mosquito midgut. *Cell. Microbiol.* **18**, 905–918 (2016).
2. R. C. Smith, J. Vega-Rodriguez, M. Jacobs-Lorena, The *Plasmodium* bottleneck: Malaria parasite losses in the mosquito vector. *Mem. Inst. Oswaldo Cruz* **109**, 644–661 (2014).
3. C. S. Hopp, P. Sinnis, The innate and adaptive response to mosquito saliva and *Plasmodium* sporozoites in the skin. *Ann. N. Y. Acad. Sci.* **1342**, 37–43 (2015).
4. Z. Shen, G. Dimopoulos, F. C. Kafatos, M. Jacobs-Lorena, A cell surface mucin specifically expressed in the midgut of the malaria mosquito *Anopheles gambiae*. *Proc. Natl. Acad. Sci. U.S.A.* **96**, 5610–5615 (1999).
5. P. Wu, P. Sun, K. Nie, Y. Zhu, M. Shi, C. Xiao, H. Liu, Q. Liu, T. Zhao, X. Chen, H. Zhou, P. Wang, G. Cheng, A gut commensal bacterium promotes mosquito permissiveness to arboviruses. *Cell Host Microbe* **25**, 101–112.e5 (2019).
6. H. Zieler, C. F. Garon, E. R. Fischer, M. Shahabuddin, Adhesion of *Plasmodium gallinaceum* ookinetes to the *Aedes aegypti* midgut: Sites of parasite attachment and morphological changes in the ookinete. *J. Eukaryot. Microbiol.* **45**, 512–520 (1998).
7. J. Tavares, P. Formaglio, S. Thiberge, E. Mordelet, N. van Rooijen, A. Medvinsky, R. Ménard, R. Amino, Role of host cell traversal by the malaria sporozoite during liver infection. *J. Exp. Med.* **210**, 905–915 (2013).
8. M. B. Heintzelman, Gliding motility in apicomplexan parasites. *Semin. Cell Dev. Biol.* **46**, 135–142 (2015).
9. D. C. Rijken, H. R. Lijnen, New insights into the molecular mechanisms of the fibrinolytic system. *J. Thromb. Haemost.* **7**, 4–13 (2009).
10. X. Bai, J. I. Weitz, P. L. Gross, Leukocyte urokinase plasminogen activator receptor and PSGL1 play a role in endogenous arterial fibrinolysis. *Thromb. Haemost.* **102**, 1212–1218 (2009).
11. M. V. Carriero, P. Franco, G. Votta, I. Longanesi-Cattani, M. T. Vento, M. T. Masucci, A. Mancini, M. Caputi, I. Iaccarino, M. P. Stoppelli, Regulation of cell migration and invasion by specific modules of uPA: Mechanistic insights and specific inhibitors. *Curr. Drug Targets* **12**, 1761–1771 (2011).
12. F. J. Castellino, V. A. Ploplis, Structure and function of the plasminogen/plasmin system. *Thromb. Haemost.* **93**, 647–654 (2005).
13. I. M. Verhamme, P. R. Panizzi, P. E. Bock, Pathogen activators of plasminogen. *J. Thromb. Haemost.* **13** (Suppl 1), S106–S114 (2015).
14. V. Ellis, K. Danø, Potentiation of plasminogen activation by an anti-urokinase monoclonal antibody due to ternary complex formation. A mechanistic model for receptor-mediated plasminogen activation. *J. Biol. Chem.* **268**, 4806–4813 (1993).

15. S. Handt, W. G. Jerome, L. Tietze, R. R. Hantgan, Plasminogen activator inhibitor-1 secretion of endothelial cells increases fibrinolytic resistance of an in vitro fibrin clot: Evidence for a key role of endothelial cells in thrombolytic resistance. *Blood* **87**, 4204–4213 (1996).
16. P. Eriksson, B. Kallin, F. M. van 't Hooft, P. Bavenholm, A. Hamsten, Allele-specific increase in basal transcription of the plasminogen-activator inhibitor 1 gene is associated with myocardial infarction. *Proc. Natl. Acad. Sci. U.S.A.* **92**, 1851–1855 (1995).
17. X. Wang, N. Wang, H. Li, M. Liu, F. Cao, X. Yu, J. Zhang, Y. Tan, L. Xiang, Y. Feng, Up-Regulation of PAI-1 and down-regulation of uPA are involved in suppression of invasiveness and motility of hepatocellular carcinoma cells by a natural compound berberine. *Int. J. Mol. Sci.* **17**, 577 (2016).
18. A. K. Ghosh, I. Coppens, H. Gårdsvoll, M. Ploug, M. Jacobs-Lorena, *Plasmodium* ookinetes coopt mammalian plasminogen to invade the mosquito midgut. *Proc. Natl. Acad. Sci. U.S.A.* **108**, 17153–17158 (2011).
19. A. K. Ghosh, M. Jacobs-Lorena, Surface-expressed enolases of *Plasmodium* and other pathogens. *Mem. Inst. Oswaldo Cruz* **106** (Suppl. 1), 85–90 (2011).
20. A. N. Vermeulen, T. Ponnudurai, P. J. Beckers, J. P. Verhave, M. A. Smits, J. H. Meuwissen, Sequential expression of antigens on sexual stages of *Plasmodium falciparum* accessible to transmission-blocking antibodies in the mosquito. *J. Exp. Med.* **162**, 1460–1476 (1985).
21. E. B. Williams, S. Krishnaswamy, K. G. Mann, Zymogen/enzyme discrimination using peptide chloromethyl ketones. *J. Biol. Chem.* **264**, 7536–7545 (1989).
22. C. Kettner, E. Shaw, Inactivation of trypsin-like enzymes with peptides of arginine chloromethyl ketone. *Methods Enzymol.* **80** (Pt. C), 826–842 (1981).
23. G. E. Blouse, K. A. Bøtkjær, E. Deryugina, A. A. Byszuk, J. M. Jensen, K. K. Mortensen, J. P. Quigley, P. A. Andreasen, A novel mode of intervention with serine protease activity: Targeting zymogen activation. *J. Biol. Chem.* **284**, 4647–4657 (2009).
24. M. L. Sanderson-Smith, Y. Zhang, D. Ly, D. Donahue, A. Hollands, V. Nizet, M. Ranson, V. A. Ploplis, M. J. Walker, F. J. Castellino, A key role for the urokinase plasminogen activator (uPA) in invasive Group A streptococcal infection. *PLOS Pathog.* **9**, e1003469 (2013).
25. A. M. De Vos, M. H. Ultsch, R. F. Kelley, K. Padmanabhan, A. Tulinsky, M. L. Westbrook, A. A. Kossiakoff, Crystal structure of the kringle 2 domain of tissue plasminogen activator at 2.4-.ANG. resolution. *Biochemistry* **31**, 270–279 (1992).
26. M. Pantzar, A. Ljungh, T. Wadstrom, Plasminogen binding and activation at the surface of *Helicobacter pylori* CCUG 17874. *Infect. Immun.* **66**, 4976–4980 (1998).
27. D. H. Petzel, H. H. Hagedorn, K. W. Beyenbach, Preliminary isolation of mosquito natriuretic factor. *Am. J. Physiol.* **249**, R379–R386 (1985).
28. C. Lahondere, C. R. Lazzari, Mosquitoes cool down during blood feeding to avoid overheating. *Curr. Biol.* **22**, 40–45 (2012).
29. J. S. Bennett, Platelet-fibrinogen interactions. *Ann. N. Y. Acad. Sci.* **936**, 340–354 (2001).
30. C. Saldanha, Fibrinogen interaction with the red blood cell membrane. *Clin. Hemorheol. Microcirc.* **53**, 39–44 (2013).
31. S. Yakovlev, L. Zhang, T. Ugarova, L. Medved, Interaction of fibrin(ogen) with leukocyte receptor $\alpha_M\beta_2$(Mac-1): Further characterization and identification of a novel binding region within the central domain of the fibrinogen γ-Module. *Biochemistry* **44**, 617–626 (2005).
32. B. Adamczyk, W. B. Struwe, A. Ercan, P. A. Nigrovic, P. M. Rudd, Characterization of fibrinogen glycosylation and its importance for serum/plasma N-glycome analysis. *J. Proteome Res.* **12**, 444–454 (2013).
33. M. Ikeda, T. Kobayashi, S. Arai, S. Mukai, Y. Takezawa, F. Terasawa, N. Okumura, Recombinant γT305A fibrinogen indicates severely impaired fibrin polymerization due to the aberrant function of hole 'a' and calcium binding sites. *Thromb. Res.* **134**, 518–525 (2014).
34. M. Martinez, J. W. Weisel, H. Ischiropoulos, Functional impact of oxidative posttranslational modifications on fibrinogen and fibrin clots. *Free Radic. Biol. Med.* **65**, 411–418 (2013).
35. E. Calvo, B. J. Mans, J. F. Andersen, J. M. C. Ribeiro, Function and evolution of a mosquito salivary protein family. *J. Biol. Chem.* **281**, 1935–1942 (2006).
36. I. M. Francischetti, J. G. Valenzuela, J. M. Ribeiro, Anophelin: Kinetics and mechanism of thrombin inhibition. *Biochemistry* **38**, 16678–16685 (1999).
37. R. Amino, S. Thiberge, B. Martin, S. Celli, S. Shorte, F. Frischknecht, R. Ménard, Quantitative imaging of *Plasmodium* transmission from mosquito to mammal. *Nat. Med.* **12**, 220–224 (2006).
38. C. S. Hughes, L. M. Postovit, G. A. Lajoie, Matrigel: A complex protein mixture required for optimal growth of cell culture. *Proteomics* **10**, 1886–1890 (2010).
39. R. H. Law, D. Abu-Ssaydeh, J. C. Whisstock, New insights into the structure and function of the plasminogen/plasmin system. *Curr. Opin. Struct. Biol.* **23**, 836–841 (2013).
40. D. A. Ayon-Nunez, G. Fragoso, R. J. Bobes, J. P. Laclette, Plasminogen-binding proteins as an evasion mechanism of the host's innate immunity in infectious diseases. *Biosci. Rep.* **38**, (2018).
41. J. González-Miguel, M. Siles-Lucas, V. Kartashev, R. Morchón, F. Simón, Plasmin in parasitic chronic infections: Friend or foe? *Trends Parasitol.* **32**, 325–335 (2016).
42. R. Lacroix, F. Sabatier, A. Mialhe, A. Basire, R. Pannell, H. Borghi, S. Robert, E. Lamy, L. Plawinski, L. Camoin-Jau, V. Gurewich, E. Angles-Cano, F. Dignat-George, Activation of plasminogen into plasmin at the surface of endothelial microparticles: A mechanism that modulates angiogenic properties of endothelial progenitor cells in vitro. *Blood* **110**, 2432–2439 (2007).
43. M. Hoylaerts, D. C. Rijken, H. R. Lijnen, D. Collen, Kinetics of the activation of plasminogen by human tissue plasminogen activator. Role of fibrin. *J. Biol. Chem.* **257**, 2912–2919 (1982).
44. R. Pannell, V. Gurewich, Activation of plasminogen by single-chain urokinase or by two-chain urokinase--a demonstration that single-chain urokinase has a low catalytic activity (pro-urokinase). *Blood* **69**, 22–26 (1987).
45. A. J. Horrevoets, H. Pannekoek, M. E. Nesheim, A steady-state template model that describes the kinetics of fibrin-stimulated [Glu^1]- and [Lys^{78}]plasminogen activation by native tissue-type plasminogen activator and variants that lack either the finger or kringle-2 domain. *J. Biol. Chem.* **272**, 2183–2191 (1997).
46. B. Arcà, F. Lombardo, C. J. Struchiner, J. M. C. Ribeiro, Anopheline salivary protein genes and gene families: An evolutionary overview after the whole genome sequence of sixteen Anopheles species. *BMC Genomics* **18**, 153 (2017).
47. H. M. O. Lester, L. l. Lloyd, Notes on the process of digestion in tsetse-flies. *Bull. Entomol. Res.* **19**, 39–60 (1928).
48. N. Simon, E. Lasonder, M. Scheuermayer, A. Kuehn, S. Tews, R. Fischer, P. F. Zipfel, C. Skerka, G. Pradel, Malaria parasites co-opt human factor H to prevent complement-mediated lysis in the mosquito midgut. *Cell Host Microbe* **13**, 29–41 (2013).
49. M. M. Castiblanco-Valencia, T. R. Fraga, A. H. Pagotto, S. M. de Toledo Serrano, P. A. E. Abreu, A. S. Barbosa, L. Isaac, Plasmin cleaves fibrinogen and the human complement proteins C3b and C5 in the presence of *Leptospira interrogans* proteins: A new role of LigA and LigB in invasion and complement immune evasion. *Immunobiology* **221**, 679–689 (2016).
50. E. I. Peerschke, W. Yin, B. Ghebrehiwet, Complement activation on platelets: Implications for vascular inflammation and thrombosis. *Mol. Immunol.* **47**, 2170–2175 (2010).
51. K. P. Sieber, M. Huber, D. Kaslow, S. M. Banks, M. Torii, M. Aikawa, L. H. Miller, The peritrophic membrane as a barrier: Its penetration by *Plasmodium gallinaceum* and the effect of a monoclonal antibody to ookinetes. *Exp. Parasitol.* **72**, 145–156 (1991).
52. R. G. Douglas, R. Amino, P. Sinnis, F. Frischknecht, Active migration and passive transport of malaria parasites. *Trends Parasitol.* **31**, 357–362 (2015).
53. M. M. Mota, G. Pradel, J. P. Vanderberg, J. C. Hafalla, U. Frevert, R. S. Nussenzweig, V. Nussenzweig, A. Rodríguez, Migration of *Plasmodium* sporozoites through cells before infection. *Science* **291**, 141–144 (2001).
54. M. Peetermans, T. Vanassche, L. Liesenborghs, R. H. Lijnen, P. Verhamme, Bacterial pathogens activate plasminogen to breach tissue barriers and escape from innate immunity. *Crit. Rev. Microbiol.* **42**, 866–882 (2016).
55. J. L. Coleman, E. J. Roemer, J. L. Benach, Plasmin-coated *Borrelia burgdorferi* degrades soluble and insoluble components of the mammalian extracellular matrix. *Infect. Immun.* **67**, 3929–3936 (1999).
56. K. Lahteenmaki, R. Virkola, R. Pouttu, P. Kuusela, M. Kukkonen, T. K. Korhonen, Bacterial plasminogen receptors: In vitro evidence for a role in degradation of the mammalian extracellular matrix. *Infect. Immun.* **63**, 3659–3664 (1995).
57. R. Virkola, K. Lahteenmaki, T. Eberhard, P. Kuusela, L. van Alphen, M. Ullberg, T. K. Korhonen, Interaction of *Haemophilus infiuenzae* with the mammalian extracellular matrix. *J. Infect. Dis.* **173**, 1137–1147 (1996).
58. D. M. Le, A. Besson, D. K. Fogg, K.-S. Choi, D. M. Waisman, C. G. Goodyer, B. Rewcastle, V. W. Yong, Exploitation of astrocytes by glioma cells to facilitate invasiveness: A mechanism involving matrix metalloproteinase-2 and the urokinase-type plasminogen activator-plasmin cascade. *J. Neurosci.* **23**, 4034–4043 (2003).
59. S. Netzel-Arnett, D. J. Mitola, S. S. Yamada, K. Chrysovergis, K. Holmbeck, H. Birkedal-Hansen, T. H. Bugge, Collagen dissolution by keratinocytes requires cell surface plasminogen activation and matrix metalloproteinase activity. *J. Biol. Chem.* **277**, 45154–45161 (2002).
60. A. Santala, J. Saarinen, P. Kovanen, P. Kuusela, Activation of interstitial collagenase, MMP-1, by *Staphylococcus aureus* cells having surface-bound plasmin: A novel role of plasminogen receptors of bacteria. *FEBS Lett.* **461**, 153–156 (1999).
61. K. Sugioka, A. Kodama-Takahshi, T. Sato, K. Okada, J. Murakami, A. M. Park, H. Mishima, Y. Shimomura, S. Kusaka, T. Nishida, Plasminogen-dependent collagenolytic properties of Staphylococcus aureus in collagen gel cultures of human corneal fibroblasts. *Invest. Ophthalmol. Vis. Sci.* **59**, 5098–5107 (2018).
62. A. Székely, D. J. Lex, Antifibrinolytics. *Heart Lung Vessel* **6**, 5–7 (2014).
63. J. Ito, A. Ghosh, L. A. Moreira, E. A. Wimmer, M. Jacobs-Lorena, Transgenic anopheline mosquitoes impaired in transmission of a malaria parasite. *Nature* **417**, 452–455 (2002).
64. S. Wang, A. K. Ghosh, N. Bongio, K. A. Stebbings, D. J. Lampe, M. Jacobs-Lorena, Fighting malaria with engineered symbiotic bacteria from vector mosquitoes. *Proc. Natl. Acad. Sci. U.S.A.* **109**, 12734–12739 (2012).
65. S. Wang, A. L. A. Dos-Santos, W. Huang, K. C. Liu, M. A. Oshaghi, G. Wei, P. Agre, M. Jacobs-Lorena, Driving mosquito refractoriness to *Plasmodium falciparum* with engineered symbiotic bacteria. *Science* **357**, 1399–1402 (2017).

66. H. Hurd, P. J. Taylor, D. Adams, A. Underhill, P. Eggleston, Evaluating the costs of mosquito resistance to malaria parasites. *Evolution* **59**, 2560–2572 (2005).
67. A. M. Feldmann, T. Ponnudurai, Selection of *Anopheles stephensi* for refractoriness and susceptibility to *Plasmodium falciparum*. *Med. Vet. Entomol.* **3**, 41–52 (1989).
68. J. Vega-Rodríguez, A. K. Ghosh, S. M. Kanzok, R. R. Dinglasan, S. Wang, N. J. Bongio, D. E. Kalume, K. Miura, C. A. Long, A. Pandey, M. Jacobs-Lorena, Multiple pathways for *Plasmodium* ookinete invasion of the mosquito midgut. *Proc. Natl. Acad. Sci. U.S.A.* **111**, E492–E500 (2014).
69. L. A. Winger, N. Tirawanchai, J. Nicholas, H. E. Carter, J. E. Smith, R. E. Sinden, Ookinete antigens of *Plasmodium berghei*. Appearance on the zygote surface of an M_r 21 kD determinant identified by transmission-blocking monoclonal antibodies. *Parasite Immunol.* **10**, 193–207 (1988).
70. E. K. Hanson, J. Ballantyne, A blue spectral shift of the hemoglobin soret band correlates with the age (time since deposition) of dried bloodstains. *PLOS ONE* **5**, e12830 (2010).
71. N. Yoshida, R. S. Nussenzweig, P. Potocnjak, V. Nussenzweig, M. Aikawa, Hybridoma produces protective antibodies directed against the sporozoite stage of malaria parasite. *Science* **207**, 71–73 (1980).
72. I. A. Quakyi, R. Carter, J. Rener, N. Kumar, M. F. Good, L. H. Miller, The 230-kDa gamete surface protein of *Plasmodium falciparum* is also a target for transmission-blocking antibodies. *J. Immunol.* **139**, 4213–4217 (1987).
73. C. S. Hopp, K. Chiou, D. R. T. Ragheb, A. M. Salman, S. M. Khan, A. J. Liu, P. Sinnis, Longitudinal analysis of *Plasmodium* sporozoite motility in the dermis reveals component of blood vessel recognition. *eLife* **4**, e07789 (2015).
74. A. Coppi, M. Cabinian, D. Mirelman, P. Sinnis, Antimalarial activity of allicin, a biologically active compound from garlic cloves. *Antimicrob. Agents Chemother.* **50**, 1731–1737 (2006).
75. G. Pradel, U. Frevert, Malaria sporozoites actively enter and pass through rat Kupffer cells prior to hepatocyte invasion. *Hepatology* **33**, 1154–1165 (2001).
76. M. Tsuji, D. Mattei, R. S. Nussenzweig, D. Eichinger, F. Zavala, Demonstration of heat-shock protein 70 in the sporozoite stage of malaria parasites. *Parasitol. Res.* **80**, 16–21 (1994).
77. A. Roth, S. P. Maher, A. J. Conway, R. Ubalee, V. Chaumeau, C. Andolina, S. A. Kaba, A. Vantaux, M. A. Bakowski, R. Thomson-Luque, S. R. Adapa, N. Singh, S. J. Barnes, C. A. Cooper, M. Rouillier, C. W. McNamara, S. A. Mikolajczak, N. Sather, B. Witkowski, B. Campo, S. H. I. Kappe, D. E. Lanar, F. Nosten, S. Davidson, R. H. Y. Jiang, D. E. Kyle, J. H. Adams, A comprehensive model for assessment of liver stage therapies targeting *Plasmodium vivax* and *Plasmodium falciparum*. *Nat. Commun.* **9**, 1837 (2018).
78. N. Singh, S. J. Barnes, R. Jenwithisuk, J. Sattabongkot, J. H. Adams, A simple and efficient method for cryopreservation and recovery of viable *Plasmodium vivax* and *P. falciparum* sporozoites. *Parasitol. Int.* **65**, 552–557 (2016).

Acknowledgments: We acknowledge the Insectary and Parasite Core Facilities of the Johns Hopkins Malaria Research Institute, The laboratory of Malaria and Vector Research at NIAID, and the Entomology Branch at Walter Reed Army Institute of Research, with special thanks to T. Savransky for production of *P. falciparum*–infected mosquitoes. The following reagent was obtained through BEI Resources, NIAID, NIH: Hybridoma 2A10 anti–*P. falciparum* CSP, MRA-183, contributed by E. Nardin. **Funding:** T.L.A.S. was supported by Conselho Nacional de Desenvolvimento Cientifico e Tecnologico (CNPq), Brazil. This research was supported by the NIH (R01AI031478 to M.J.-L.), (R01 AI132359 to P.S.), the Johns Hopkins Malaria Research Institute Insectary and Parasite Core Facilities, the Bloomberg Philanthropies, the Military Infectious Disease Research Program (Q0480_19_WR_CS_OC to B.S.P), the NIH Distinguished Scholars Program, and the Intramural Research Program of the Division of Intramural Research AI001250-01, NIAID, NIH. Supply of human blood was supported by the NIH grant RR00052.
Author contributions: Conceptualization: T.L.A.S., J.V.-R., and M.J.-L. Methodology: T.L.A.S., J.V.-R., P.H.A., A.Ra., A.B., A.Ro., H.B., and M.J.-L. Investigation: T.L.A.S, J.V.-R., P.H.A, A.Ra., A.B., T.V.P., Z.R.P., A.Ro., Y.J.J, J.O., A.K.G., and H.B.; Formal Analysis, T.L.A.S., J.V.-R., P.H.A, A.Ra., A.B., T.V.P, Z.R.P., A.Ro., Y.J.J., J.O., A.K.G., and H.B. Writing—original draft: T.L.A.S., J.V.-R., and M.J.-L.; Writing—review and editing: T.L.A.S, J.V.-R., P.H.A., A.Ra., A.B., T.V.P., Z.R.P., A.Ro., Y.J.J., J.O., A.K.G., H.B., B.S.P., P.S., and M.J.-L. Visualization: T.L.A.S., J.V.-R., and M.J.-L. Funding acquisition: J.V.-R., B.S.P., P.S., and M.J.-L. Supervision: J.V.-R., B.S.P., P.S., and M.J.-L. **Competing interests:** The authors declare that they have no competing interests. **Data and materials availability:** All data needed to evaluate the conclusions in the paper are present in the paper and/or the Supplementary Materials. Additional data related to this paper may be requested from the authors. The hybridoma cell line 2A10 anti–*P. falciparum* CSP, MRA-183, can be obtained from BEI Resources (www.beiresources.org) pending scientific review and a completed material transfer agreement.

Submitted 14 August 2020
Accepted 21 December 2020
Published 5 February 2021
10.1126/sciadv.abe3362

Citation: T. L. Alves e Silva, A. Radtke, A. Balaban, T. V. Pascini, Z. R. Pala, A. Roth, P. H. Alvarenga, Y. J. Jeong, J. Olivas, A. K. Ghosh, H. Bui, B. S. Pybus, P. Sinnis, M. Jacobs-Lorena, J. Vega-Rodríguez, The fibrinolytic system enables the onset of *Plasmodium* infection in the mosquito vector and the mammalian host. *Sci. Adv.* **7**, eabe3362 (2021).